Software Interface Specification for the Hayabusa2 Optical Navigation Camera (ONC) Data Products

Version 1.0

October 27, 2022

Prepared by

Rie Honda[1], Manabu Yamada[2], M. Katherine Crombie[3], Yukio Yamamoto[4], Shin-ya Murakami[4], Toru Kouyama[5], Eri Tatsumi[6,9], Yasuhiro Yokota[4], Shingo Kameda[7], Hidehiko Suzuki[8], Tomokatsu Morota[9], Moe Matsuoka[4], Yuichiro Cho[9], Naoya Sakatani[7], Hirotaka Sawada[4,] Kazunori Ogawa[4], Chikatoshi Honda[10], Masahiko Hayakawa[4], Kazuo Yoshioka[9], Koki Yumoto[9], Seiji Sugita[9]

1 Ehime University
2 Chiba Institute of Technology
3 Indigo Information Services
4 Japan Aerospace Exploration Agency
5 National Institute of Advanced Industrial Science and Technology
6 Instituto de Astrofísica de Canarias
7 Rikkyo University
8 Meiji University
9 The University of Tokyo
10 The University of Aizu

Table of Contents

Change Log

DATE	CHANGE	AFFECTED SECTIONS
2017-11-06	Initial Draft	All
2017-12-01	Second Draft	All
2018-03-30	Third Draft	All
2020-10-23	Forth Draft	All
2021-05-01	Fifth Draft	All
2021-07-06	Sixth Draft	All
2022-02-25	Seventh Draft	All
2022-10-27	Version 1.0	All

Acronyms and Abbreviations

Acronym/Abbreviation	Definition
A/D	Analog to Digital
AOCS	Attitude and Orbit Control System
ASCII	American Standard Code for Information Interchange
CCD	Charge-Coupled Device
CK	Orientation or Attitude kernel (“C-Matrix” kernel)
DAC	Data Archive team
DE	Digital Electronics
DN	Digital Number
DR	Data Recorder
ECAS	Eight Color Asteroid Survey
FF (lamp)	Flatfield (lamp)
FFT	Fast Fourier Transform
FITS	Flexible Transport Image System
FK	Frames kernel
FOV	Field Of View
FWHM	Full Width Half Maximum
HDU	Header Data Unit
HK	House Keeping (packet)
HP	Home Position
IAU	International Astronomical Union
I/F	Radiance factor
IK	Instrument kernel
IPDA	International Planetary Data Alliance
ISAS	Institute of Space and Astronautical Science
JAXA	Japan Aerospace Exploration Agency
LIDAR	Light Detection And Ranging
LSK	Leapseconds kernel
MASCOT	Mobile Asteroid surface SCOuT
MINERVA-II	MIcro Nano Experimental Robot Vehicle for Asteroid the Second Generation
NAIF	Navigation and Ancillary Information Facility
ND	Neutral Density
NDVI	Normalized Difference Vegetation Index
OB	Optical Black
ONC	Optical Navigation Camera
ONC-AE	ONC Analogue Electronics
ONC-E	ONC Digital Electronics

Acronym/Abbreviation	Definition
ONC-T	Optical Navigation Camera – Telescope
ONC-W	Optical Navigation Camera – Wide-angle
PCK	Planetary Constants kernel
PDS	Planetary Data System
PSF	Point Spread Function
RGB	Color space using red, green, and blue.
RMS	Root mean square
ROI	Region of Interest
SBN	Small Bodies Node
S/C	Spacecraft
SCI	Small Carry-on Impactor
SCLK	Spacecraft Clock Kernel
SfM	Structure-from-Motion
SIRIUS	Scientific Information Retrieval and Integrated Utilization System
SIS	Softwares Interface Specification
SPC	Stereophotoclinometry
SPICE	Spacecraft, Planet, Instrument, C-Matrix, Events
SPK	Ephemeris data kernel
SURF	Speeded Up Robust Features
TD1	The first touchdown
TD2	The second touchdown
TI	Time Indicator
UTC	Coordinated Universal Time
UV	Ultraviolet
XML	Extensible Markup Language

1 Purpose and Scope of Document

The purpose of this Data Product Software Interface Specification (SIS) is to provide users of the raw, calibrated, and derived data products from the Hayabusa2 Optical Navigation Camera (ONC) with a detailed description of the products, and a description of the product generation procedures, including data sources and destinations. The products defined in this document are raw, partially processed, calibrated, and co-registered (spatially aligned) multi-band images. The calibration, browse, and geometry products, are also defined. The images are generally of (162173) Ryugu but may be of other targets of opportunity.

The SIS is intended to provide enough information to enable users to read and understand the ONC data products as stored in the Planetary Data System (PDS). The users for whom this SIS is intended are software developers of the programs used in generating the ONC products and scientists who will analyze the data, including those associated with the Hayabusa2 mission, ONC instrument, and those in the general planetary science community.

2 Applicable Documents

This SIS is consistent with the following Planetary Data System Documents as adopted by the International Planetary Data Alliance (IPDA):

1. Planetary Data System Standards Reference, Version 1.14.0, May 22, 2020.
2. PDS4 Data Dictionary – Abridged – Version 1.14.0.0, March 23, 2020.
3. PDS4 Information Model, Version 1.14.0.0, March 23, 2020.

This SIS is responsive to the following Hayabusa2 mission document(s):

4. Science Policy for Hayabusa2 Project, Version 3.0, May 14, 2018.

This SIS makes reference to the following documents:

5. Kameda, S. et al., Preflight Calibration Test Results for Optical Navigation Camera Telescope (ONC-T) Onboard the Hayabusa2 Spacecraft, *Space Science Reviews,* **208**, 17-31, https://doi.org/10.1007/s11214-015-0227-y, 2017.
6. Suzuki, H. et al., Initial inflight calibration for Hayabusa2 optical navigation camera (ONC) for science observations of asteroid Ryugu, *Icarus*, **300**, 341-359, https://doi.org/10.1016/j.icarus.2017.09.011, 2018.
7. Tatsumi, E. et al., Updated inflight calibration of Hayabusa2's optical navigation camera (ONC) for scientific observations during the cruise phase, *Icarus*, **325**, 153-195, https://doi.org/10.1016/j.icarus.2019.01.015, 2019a.
8. Tatsumi, E. et al., Updated flat-fields of ONC-T/Hayabusa2 based on close encounter with Ryugu, *50th Lunar and Planetary Science Conference 2019*, #1743, pp. 2, 2019b.
9. Tatsumi, E. et al., Global photometric properties of (162173) Ryugu, *A&A*, **639**, A83, https://doi.org/10.1051/0004-6361/201937096, 2020.
10. Kouyama, T. et al., Post-arrival calibration of Hayabusa2's optical navigation cameras (ONCs): Severe effects from touchdown events, *Icarus*, **360**, 114353, https://doi.org/10.1016/j.icarus.2021.114353, 2021a.
11. Kameda, S. et al., Improved method of hydrous mineral detection by latitudinal distribution of 0.7-μm surface reflectance absorption on the asteroid Ryugu, *Icarus*, **360**, 114348, https://doi.org/10.1016/j.icarus.2021.114348, 2021.

Complete list of the references is found at Appendix 8.1.

3 Configuration Management

The Hayabusa2 ONC team controls the data products described in this document, as well as the document itself. Requests for changes to the data products or the document's scope and contents are made to the Hayabusa2 ONC team principal investigator, Seiji Sugita. An engineering change request will be evaluated against its impact on the ONC ground data processing system before acceptance. Once a change request has been approved, software and documentation are updated, version numbers incremented, tested, and finally released for production.

The data products and documentation described in this SIS as well as the SIS itself have completed a formal PDS peer review and lien resolution process. The peer review ensures that all data products described by this SIS comply with PDS4 standards as noted in Section 2 – Applicable Documents. The PDS peer review panel consisted of members of the PDS Small Bodies Node (SBN) and of the planetary science community. Any changes to data products subsequent to the peer review, will be reviewed internally by the PDS SBN to determine if an additional peer review is necessary.

4 Relationships with Other Interfaces

Changes to the data products described in this SIS affect the following software, products or document as shown in Table 1. A systems engineering approach is used to evaluate how changes in any one of these interfaces affect the others. It is possible that changes to one of these items will not affect any other item.

Table 1 Interface relationships

Name of Interface	**Type**	**Owner**
ONC Database Schema	Product	ONC Team
ONC Raw Science Data	Product	ONC Team
ONC Raw Housekeeping Data	Product	ONC Team
ONC Calibrated Science Data	Product	ONC Team
Science Policy for Hayabusa2	Document	Project
ONC Ground Data Processing	Software	ONC Team
ONC Archive Software	Software	DAC Team

5 Data Product Characteristics and Environment

5.1 Instrument Overview

The Hayabusa2 Optical Navigation Camera (ONC) system comprises one telescopic camera (ONC-T) and two wide-angle cameras (ONC-W1 and ONC-W2). Figure 1 shows a schematic view of the Hayabusa2 spacecraft and ONC camera suite. The definition of image coordinates and their relationship to the spacecraft coordinate system for the three cameras are illustrated in Figure 2. The cameras are controlled using a common electronics device (ONC-AE). The camera system is operated mainly in the approach phase and the asteroid proximity phase. In the former phase, the ONC system is used to navigate the spacecraft to asteroid (162173) Ryugu. After arrival at Ryugu, a digital terrain model will be developed based on the image data obtained with the ONC. The ONC-T has a wheel with seven bandpass filters, allowing the team to obtain a global spectral map of Ryugu.

The terrain model and the global spectral map are important for both characterizing the asteroid and selecting touchdown sites for sampling. The visible wavelength range, covered by the ONC-T possesses a number of key spectroscopic quantities, such as albedo, spectral slope in the UV to short visible range, and 0.7-μm absorption band, important for characterizing mineralogical and physical properties of asteroid (e.g., Rivkin et al., 2004; Sugita et al., 2013).

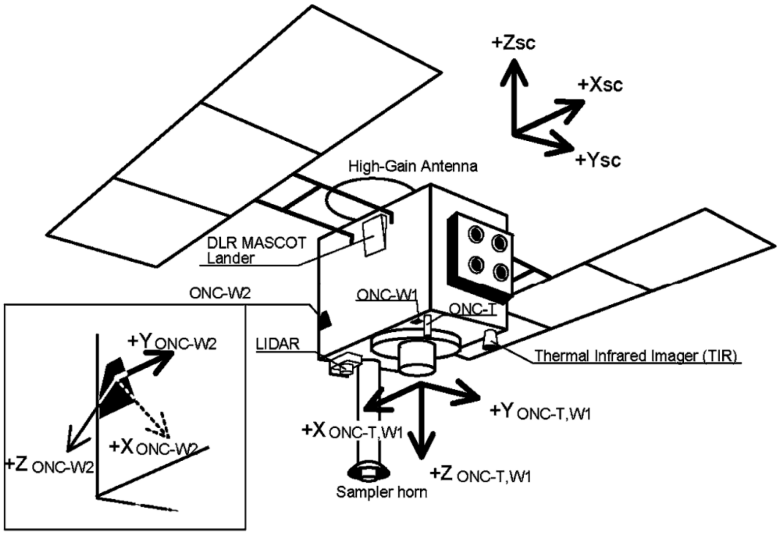

Figure 1 A schematic view of the Hayabusa2 spacecraft and ONC camera suites; ONC-T, ONC-W1 and ONC-W2. This figure is reproduced from Kameda et al., 2017.

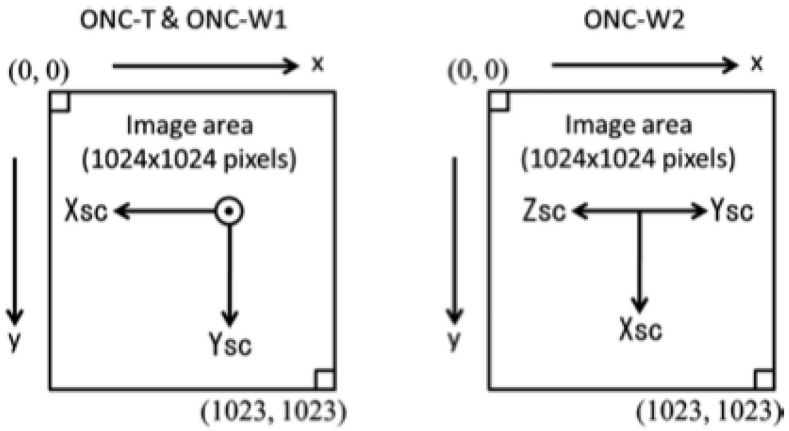

Figure 2 Definition of image coordinate system for (left) ONC-T, ONC-W1 and (right) ONC-W2. Xsc, Ysc, and Zsc indicate the spacecraft coordinate system (For definition, see Figure 1). Since the center of FOV is slanted from nadir direction, none of the spacecraft axes (Xsc, Ysc, and Zsc) are normal to CCD of ONC-W2. This figure is reproduced from Suzuki et al., 2018.

5.1.1 ONC-W1 and -W2

ONC-W1 and W2 are wide view (>65 deg × 65 deg) panchromatic charge-coupled-device (CCD) cameras mainly used for optical navigation during cruise and low-altitude operations near the asteroid. Figure 3 shows the appearance of ONC-W1 and ONC-W2. The design for the two cameras is almost identical except for the transmittance of the neutral-density (ND) filter and the viewing direction relative to the spacecraft. The center of view of ONC-W1 was aligned in the –Z direction of

the spacecraft coordinate system (i.e., nadir viewing), while that of the ONC-W2 was slanted by approximately 30 degrees from the –Z direction. Since both ONC-W1 and W2 are in focus from a short distance, both cameras are expected to obtain detailed images of the surface of Ryugu during touch down procedures. Technical specifications for ONC-W1 and W2 taken from Suzuki et al. (2018) can be found in Table 2.

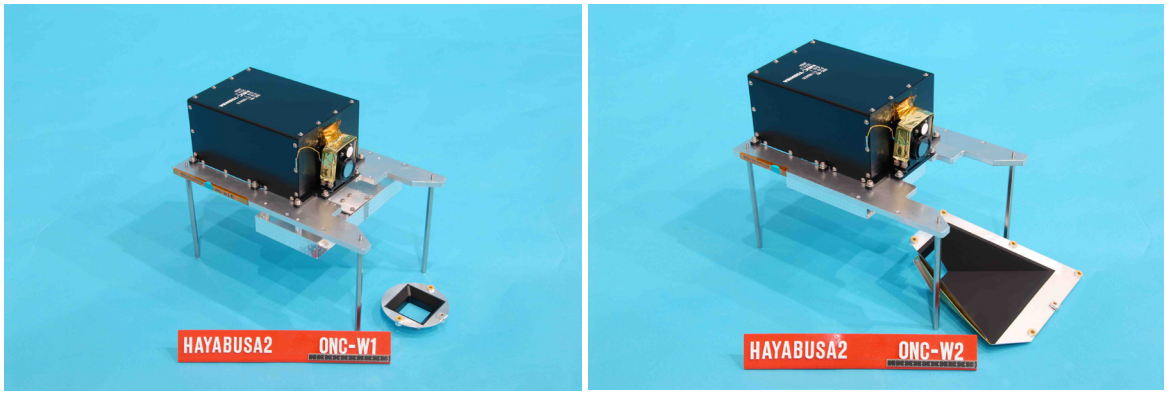

Figure 3 The appearance of ONC-W1 (left) and ONC-W2 (right).

5.1.2 ONC-T

The ONC-T is a telescopic CCD camera with a line of sights along the −Z direction in the spacecraft coordinate system. Figure 4 shows the appearance of ONC-T. The focal length is 120.50 mm, and the pixels are 13 μm × 13 μm in size. Thus, the angular pixel resolution is 22.14 arcsec/pixels or 0.1 mrad/pixels. The CCD image sensor has an active area of 1024 × 1024 pixels, and the field of view (FOV) is 6.27° × 6.27°. Thus, a 2 km × 2 km area can be imaged with ONC-T from the home-position (HP) altitude of 20 km, with a pixel resolution of 2 m/pixels. At 100 m of altitude, a 10 m × 10 m area can be observed with each frame, with a pixel resolution of 10 mm/pixels.

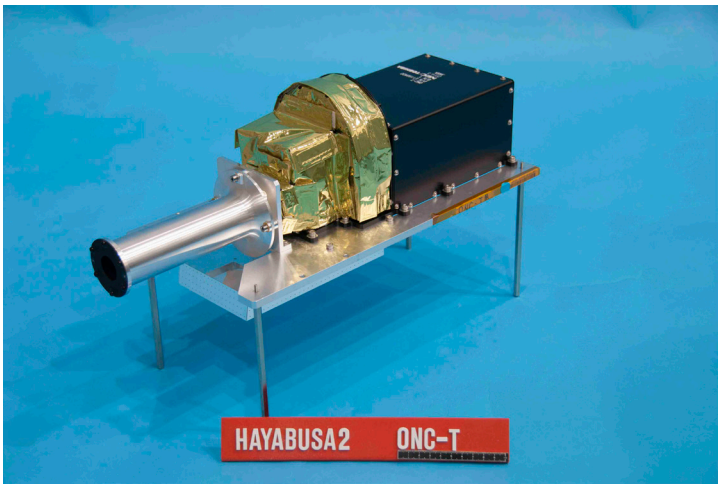

Figure 4 The appearance of ONC-T.

The ONC-T has a wheel with seven bandpass filters and a panchromatic window for the correction of the light path length (Kameda et al., 2015). The center wavelength and the approximate value of bandwidth of the filters are (390 nm, 40 nm) for ul-band, (480 nm, 30 nm) for b-band, (550 nm, 30 nm) for v-band, (589 nm, 10 nm) for Na, (700 nm, 30 nm) for w-band, (860 nm, 30 nm) for x-band, and (950 nm, 60 nm) for p-band. These filters except for 'Na' were selected based on the filters used

by the Eight Color Asteroid Survey (ECAS) (Zellner et al., 1985) although the central wavelengths of both ul- and b-bands have been shifted long ward to fit in the sensitive spectral range of the CCD. The transmittance of the panchromatic window (wide) is constant (~95 %) in the spectral range of 300 to 1200 nm. Technical specifications for ONC-T taken from Kameda et al. (2017) can be found in Table 2. Figure 5, Figure 6, and Figure 7 show the flatfields obtained in pre-launch calibration, system efficiency of ONC-W1, W2, and system efficiency of each band of ONC-T, respectively. Additional details about the ground and inflight calibrations of the ONC sensors can be found in the instrument calibration papers (Kameda et al., 2017, Suzuki et al., 2018, Tatsumi et al., 2019a, and Kouyama et al., 2021a).

Table 2 Summary of technical specifications of ONC-W1, -W2, and -T.

Parameter	ONC-W1 and ONC-W2	ONC-T
F number	9.6	9.05 (Effect of FF lamp included)
Effective aperture diameter	1.08 mm	15.1 mm
Focal length	W1:10.22 mm W2:10.38 mm	120.50 mm [1]
Field of view (Optical black pixels are excluded)	W1: 69.71° (nadir view) W2: 68.89° (slanted ~30° from nadir)	6.27° × 6.27°
CCD array size	1056 (H) × 1024 (V) pixels (16 × 1024 pixels on both sides are Optical Black pixels)	1056 (H) × 1024 (V) pixels (16 × 1024 pixels on both sides are Optical Black pixels)
CCD pixel size	13 μm × 13 μm	13 μm × 13 μm
Mean pixel resolution	W1: 0.06808°/pixel W2: 0.06728°/pixel	0.00612°/pixel
Filters (turn-over rate)	Not applicable	7 narrow-bands and 1 wide-band, 1: ul, 2: wide, 3: v, 4: w, 5: x, 6: Na, 7: p, and 8: b. (4.69 s/filter)
Transmittance of ND filter	W1: 7% W2: 20%	28 – 35 %
Sensitivity flatness [2]	W1: 67.3% and 72.0% at corners of FOV W2: 82.8% and 82.8% at corners of FOV, See Figure 5.	About 20% at corners of FOV. See Figure 5.
System efficiency	See Figure 6.	See Figure 7.
Pixel sampling rate	3 MHz	3 MHz
A/D conversion	12-bit, 10-bit, 8-bit (via division in DE or ONC-E)	12-bit, 10-bit, 8-bit (via division in DE or ONC-E)
Gain factor	W1:20.86 e^-/COUNT, W2:20.11 e^-/COUNT	20.95 e^-/COUNT
Dark signal (e-/pixel/sec) at 20 degC [3]	W1:279, W2:304	261
Readout noise(e-)	W1:36.3, W2: 37.0	38.5
PSF(FWHM) [pixel]	W1:0.45, W2:0.45	0.24 – 0.34

[1] The value in Kameda et al. (2017) was 121.1 mm. The value was re-determined to be consistent with the distortion (Tatsumi et al., 2019a).
[2] Values normalized by sensitivity at center of FOV.
[3] On Catalogue: $Q_{\mathrm{d}}/Q_{\mathrm{d0}} = 1.14 \times 106\, T^3 \exp(-9080/T)$, where Q_{d0} is dark signal at 20 degC and Q_{d} is dark signal at T degC.

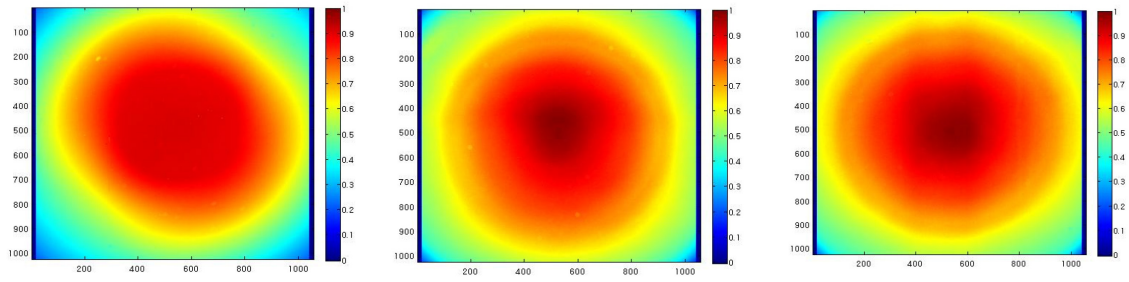

Figure 5. Examples of flatfield images (left: ONC-T v-band, center: ONC-W1, right: ONC-W2, obtained on integration sphere on March 26th, 2014 (data set "version 1" in Table 27).

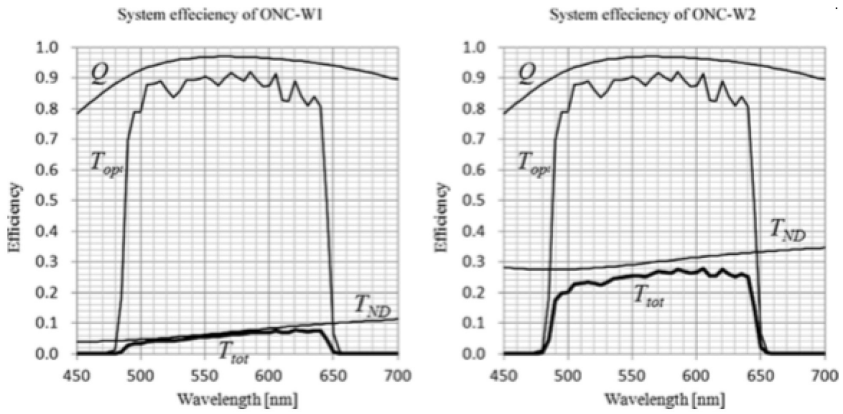

Figure 6. System efficiencies of ONC-W1 (left) and ONC-W2 (right). Quantum efficiency, Q (number of photoelectrons per single photon), the transmittance T_{OPT} of the optical system and the transmittance T_{ND} of neutral density filter, and the total transmittance T_{tot} of the entire camera system are shown in the figure (Suzuki et al., 2018).

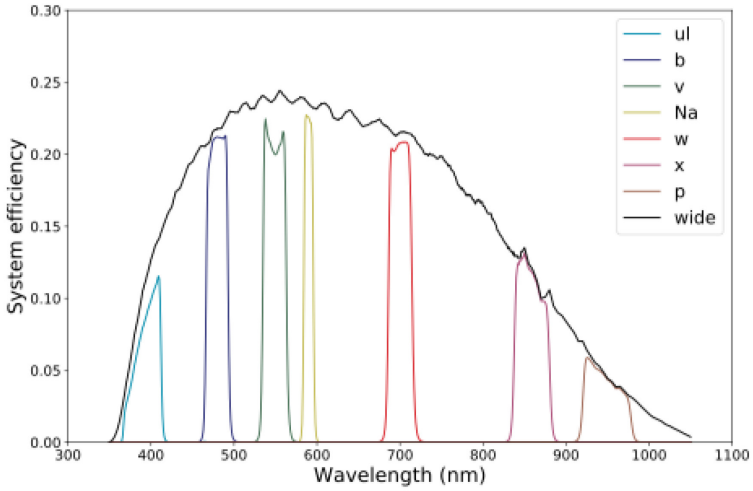

Figure 7. System efficiency of each band of ONC-T as the products of transmittance of lens system, ND filter, band-pass filter (except for wide), and quantum efficiency of CCD (Tatsumi et al., 2019a).

5.1.3 Onboard Data Processing

Figure 8 shows the configuration of pixels in a sensor. The original image size is 1056 pixels × 1024 pixels, and the 16-pixel band-like regions are "optical black" where no light directly strikes the pixels. The area of 1024 pixels × 1024 pixels in the center is extracted and used as a normal frame image. As shown in Figure 8, the original image is divided into a normal image and two optical black areas and rearranged as a frame image and an optical black image in which both of left and right optical black areas are merged into a single image of 32 pixels × 1024 pixels. Obtained images are stored in the pre-processing buffer of instrument Digital Electronics (DE) temporarily and processed and/or compressed and sent to Data Recorder (DR) and stored there for downlink transmission. Optical black images are downlinked only for special purpose analysis such as bias check.

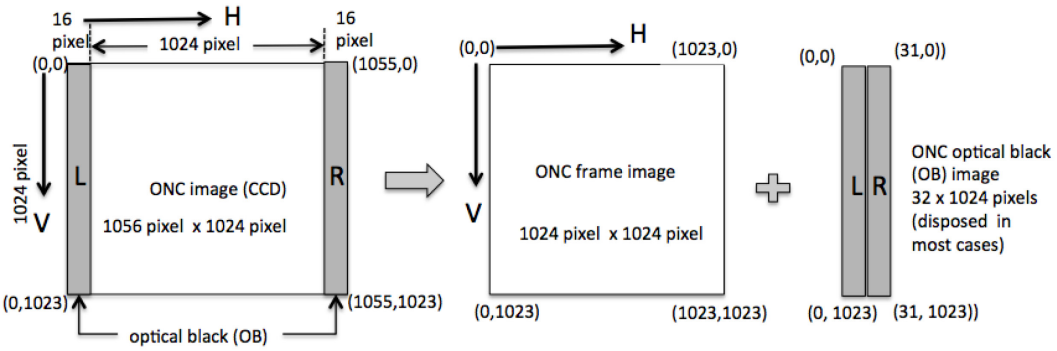

Figure 8. Relationship between ONC original image, ONC frame image and optical black image.

Table 3 summarizes the types of image processing conducted in the DE for the original 12-bit ONC images. Smear and bias reduction (subtraction of a zero-exposure image from a target image), binning, bit reduction, region of interest (ROI) selection, and compression are conducted as required. Original image has a bit depth of 12-bits, although data are treated as signed 16-bit integer during processing in the DE.

Table 3. Image processing conducted onboard at DE.

Operation	Detail
Smear and bias reduction	Smear noise and bias are reduced by subtracting an image with zero exposure time from non-zero exposure time image. Two images are taken consecutively.
Binning	2 × 2, 4 × 4, 8 × 8 binning.
Bit depth reduction	Reduction of bit depth is conducted onboard by using division operation in the DE. 10-bit and 8-bit images are created by division by 4 and 16, respectively. Each pixel is still an unsigned 16-bit integer, however this operation improves the efficiency of compression and increases the compression ratio.
Compression (ROI selection included)	Lossless compression (StarPixel Lossless) or Lossy compression (StarPixel Flexible) is conducted for 16384 pixels in both each block of 128 × 128 pixels in a frame image and 16 × 1024 pixels in an optical black image. During this process, a region of interest (ROI) is specified. Multiple blocks can be specified for selection of the ROI, however, the selected area must be a consecutive rectangle in the image coordinate as shown in Figure 9(3).

Figure 9 shows schematic views of each processing in the DE listed in Table 3. Bias and smear noise reduction is conducted for most images onboard to reduce the amount of data. This process is skipped in some cases where a long exposure time is required for imaging of dark targets or in a case there is no time for onboard calibration before the next imaging starts. Also binning and bit depth

reduction can be conducted onboard by using functions of the DE. The images are divided into blocks of 128 pixels × 128 pixels, and each block is compressed by a lossless compression (StarPixel Lossless) or a lossy compression (StarPixel Flexible) algorithm. During the compression, regions of interest (ROI) can be selected. Multiple blocks can be specified during this process, however only consecutive blocks can be specified as shown in Figure 9(3).

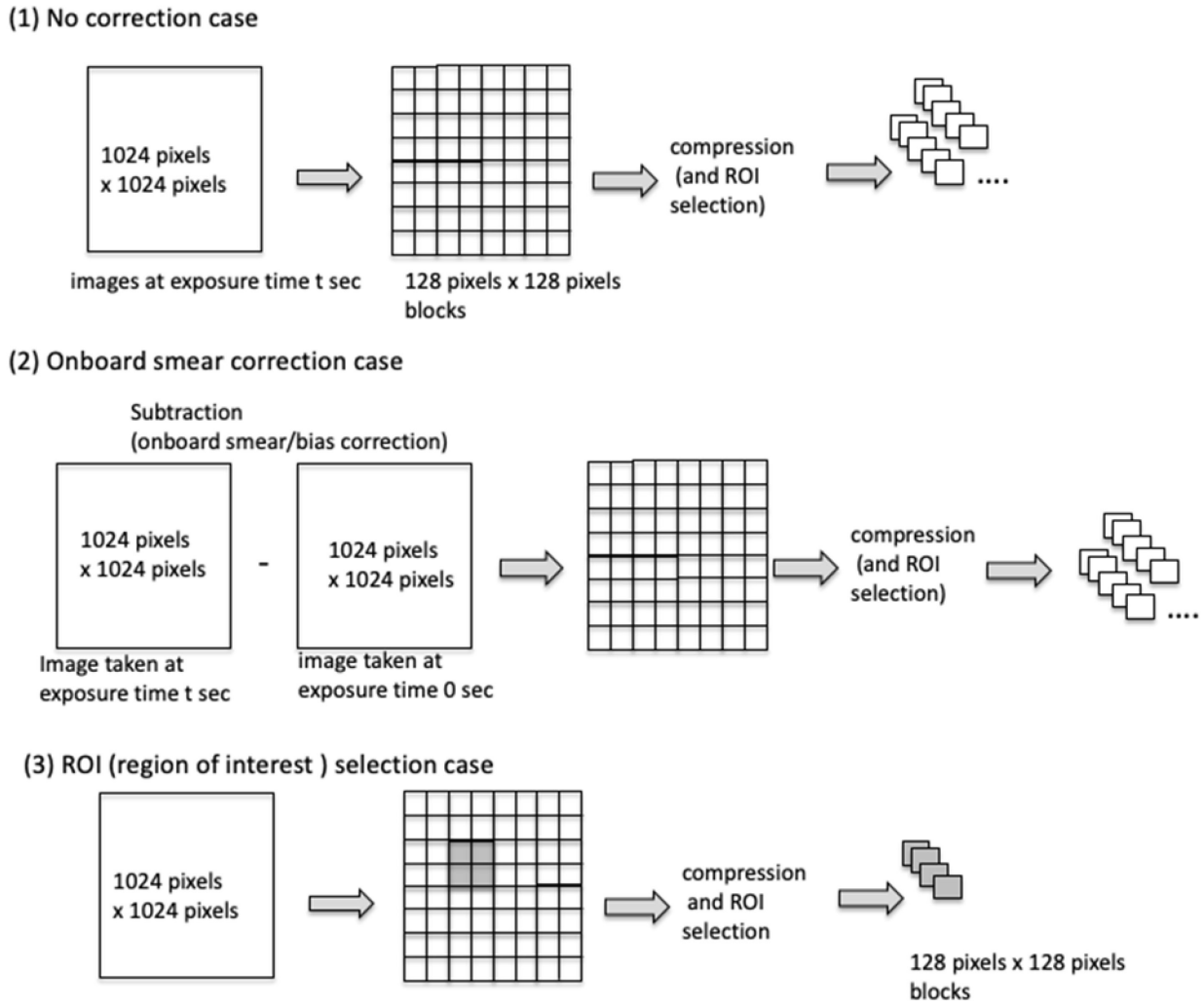

Figure 9. Overview of image processing on the spacecraft.

Table 4 summarizes image processing types. Most of the images obtained in the proximity phase are “Ryugu for spectral analysis” or “Ryugu for morphological analysis” type images.

Table 4. Typical image processing conducted onboard.

Purpose or target	Smear noise reduction	Bit depth conversion	Compression	ROI selection	Binning
Calibration, health check	Yes / No	12 or 10	Lossless	Some	None
Star and planet observation	No	12	Lossless	Some	None
Ryugu for spectral analysis	Yes / No [1]	10	Lossless	Not used	None
Ryugu for morphological analysis	Yes / No [1]	8	Lossy	Not used	None
Na atmosphere observation	No	12[2]	Lossless	Not used	4×4 or 8×8
Onboard stacked observation	No	12[2]	Both	Not used	None

[1] Onboard smear noise reduction was skipped for images taken just before and after touchdown at the altitude less than 200 m.
[2] This value is the bit depth of raw image. The bit depth up to 16 is available for onboard binning or stacking. Thus, the signals of these type of images are divided by the number of binned pixels or stacked images during L2b creation.

5.2 Data Product Overview

The ONC data products are raw, calibrated, derived mosaic images, and associated backplane data of the surface of Ryugu. The images will be used to measure asteroid shape, local morphologies, and visible spectroscopic properties of the asteroid. All ONC image data are formatted natively as Flexible Transport Image System (FITS) data, with images stored as arrays, and metadata captured in the image headers. All metadata needed to use or interpret the images is duplicated in the PDS4 XML labels.

The ONC data products are:

1. **ONC Raw / Partially Onboard Processed Image Data**: Images that have been reassembled from downlinked telemetry with complete image metadata including instrument settings, states, and geometry. Smear noise and bias are removed onboard for most images but not all images are corrected.
2. **ONC Partially Processed Image Data**: Images that have been corrected for instrumental noise, flatfield, and stray light. If smear and bias correction is not performed onboard, these processes are conducted in this level. Temperature dependences of bias and flatfield pattern are also corrected, and signals are finally calibrated to the value in counts, that corresponds DN at 12-bits.
3. **ONC Distortion Corrected and Physically Converted Image Data:** Images that have been corrected for camera distortion effects and calibrated into physical radiance units ($W/m^2/\mu m/str$) with complete image metadata including instrument settings, states in physical units, and corresponding observation geometry. The CCD temperature dependence of the sensitivity is considered while creating this product.
4. **ONC Derived I/F Image Data**: Images that have been calibrated to radiance factor (I/F) by dividing the estimated irradiated signal by the irradiance of the Sun.
5. **ONC Derived Photometrically Corrected Reflectance Image Data**: Bidirectional reflectance images at the standard viewing condition that have been photometrically corrected using the Hapke's function and the shape model. Viewing geometry parameters such as incident angle, emission angle and solar phase angle are calculated by using a shape model and spacecraft trajectory and used for the correction. Used viewing geometry parameters are stored in ONC Derived Backplane Image Cube Data.

6. **ONC Derived Backplane Image Cube Data**: Backplane data created for each pixel of Derived I/F Image Data that include longitude, latitude, and viewing geometry parameters (incident angle, emission angle, solar phase angle, polygon id, and distance from the facet). The dataset is natively stored in a fits cube format. This data is created by using the software called plate_renderer (Hirata, 2018).
7. **ONC Derived Co-Registered I/F Image Cube Data:** The I/F image set co-registered to the specific band image. The reference band is set to be the temporal middle band in the sequence of multi-band imaging to minimize the shift of the images.
8. **ONC Derived Co-Registered Photometrically Corrected Reflectance Image Cube Data**: The I/F image set co-registered to the specific band image.
9. **ONC Calibration Data Product**: The data used for calibration.
10. **ONC Browse Product**: Quick look image product for data in other collections.

The current SIS describes only Raw image, Partially Processed image, Calibrated images Distortion Corrected and Physically Converted image, and Co-Registered image cube. The other products such as mosaicked map will be documented in the future or in the other SIS related to map.

5.3 Data Processing

This section of the SIS provides general information about data product content, format, size, and production rate. The specifics of the data product formats are discussed in Section 6.

5.3.1 Data Processing Level

ONC will deliver raw, partially processed, calibrated, and derived image data to PDS. Table 5 describes the processing level of each product in both Hayabusa2 project terms and PDS4 terms. Definitions of the PDS4 processing levels can be found in Appendix 8.2.

Table 5. ONC data products and their processing levels

ONC Product	**PDS4 Processing Level**	**ONC Processing Level**
Raw / Partially Onboard Processed Image Data	Raw	L2a
Partially Processed Image Data	Partially Processed	L2b
Distortion Corrected and Physically Converted Image Data	Calibrated	L2c
Derived I/F Image Data	Derived	L2d
Derived Photometrically Corrected Reflectance Image Data	Derived	L2e
Derived Co-Registered I/F image Cube Data	Derived	L2drc
Derived Co-Registered Photometrically Corrected Reflectance Image Cube Data	Derived	L2erc
Derived Backplane Image Cube Data	Derived	L2dbpc
Calibration Data	Derived	--
Browse Product	Derived	--

5.3.2 Data Product Generation

5.3.2.1 Level 2a – Raw / Partially Onboard Processed Image Data

Images processed and compressed by an onboard computer are downlinked from the spacecraft as separated block images and stored as sorted telemetry in the Scientific Information Retrieval and Integrated Utilization System (SIRIUS) database at ISAS/JAXA. The downlinked block images are decompressed and merged into an original frame image in FITS format by the ONC pipeline tool. Spacecraft system housekeeping (HK) data and ONC status data are downlinked together with an image data. The temperatures of the ONC sensor, lens system, and electronics, as well as the voltages of the electronics are calculated by averaging HK data between closet time before the start time of imaging and closest time after the end time of imaging. ONC status data are taken at the time of imaging. These data are attached to the FITS image header. As described in Section 5.1.3, most of the restored images are onboard-smear-corrected images, however some raw images for calibration or long exposure time observation without onboard smear-correction are included. Furthermore, some images are stacked or binned onboard.

The final level 2a (L2a) image data is a FITS file with two HDUs (Header Data Unit) containing metadata as a header and a data of raw or onboard-corrected data of either main area (1024 pixels × 1024 pixels) or optical black (32 pixels × 1024 pixels). The size of some of main area images are less than 1024 pixels × 1024 pixels due to binning or extraction of ROI. The unit of data is DN.

Geometry related FITS header keywords that have the prefix S_ such as S_DISTHR were calculated using the Hayabusa2 SPICE kernels without LIDAR derived SPK and SPK obtained as a by-product of shape model. Filenames of the SPICE kernels used to calculate the FITS header keywords with the prefix S_ were written as COMMENT lines starting with “BEGIN SPICE KERNELS” and ended with “END SPICE KERNELS”. Geometry related FITS header keywords that have the prefix M_ such as M_FCLAT are about geometry of Ryugu. Longitudes and latitudes of center of image and at the four corner pixels of image are described in M_FCLAT, M_FCLON, M_4CNLAT, and M_4CNLON. Distance between the spacecraft and Ryugu at the center of image is described in M_FCDIST, and the horizontal spatial resolution of image at the surface of Ryugu is described in M_FCRES. These values were extracted from the l2dbpc product, which filename is described in M_BPFIL. The l2dbpc product described in M_BPFIL was created using SPICE kernels described in M_MKERN1, M_MKERN2, M_MKERN3, and M_DSK. Usually, M_MKERN1, M_MKERN2, and M_MKERN3 specified the meta kernel using the LIDAR derived SPK or the SPK obtained as a by-product of shape model. The ONC team manually determined a better meta-kernel for each image by visual inspection. Note that after NAIF’s review of the Hayabusa2 SPICE Archive bundle, some of the filenames were changed. In the XML label, changed filenames were referred so that one can directly refer the archived SPICE kernels without conversion from the original filename to the archived filename.

5.3.2.2 Level 2b – Partially Processed Image Data

In the Level 2b product, effects of the camera hardware and imaging conditions, such as exposure time, smear, and CCD temperature dependence of bias and flatfield pattern, are corrected. The overview of the calibration flow is shown in Figure 10. Bit depth correction, bias reduction, radiator stray light removal, non-linearity correction, dark current removal, hot pixel correction (not conducted currently), and smear noise reduction are preformed successively on raw images, where bias and smear noise reductions are skipped if the onboard smear correction was already performed. The effect of vignetting and non-uniform sensitivity is then corrected by dividing the image by the flatfield data normalized at the center of FOV.

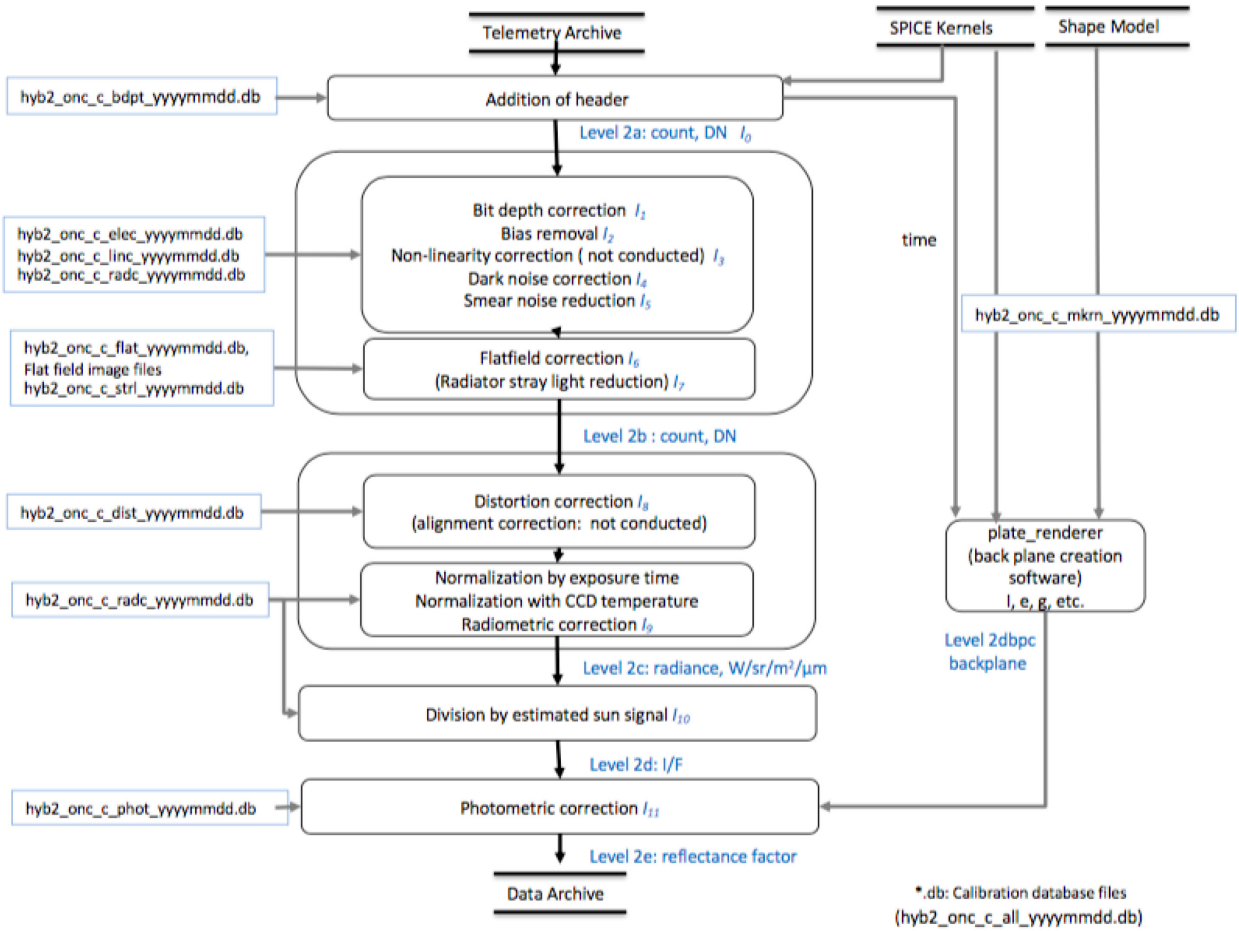

Figure 10. The overview of calibration flow. Bias removal and smear noise reduction are skipped for onboard smear corrected images.

The final level 2b (L2b) data is a FITS file with two HDUs containing metadata as headers and a Partially Processed Image Data in counts that is DN converted to 12-bits. The L2b data doesn't contain optical black data.

The detailed processes of calibration steps are described as follows. Note that all parameters of the calibration equation in the following sections are summarized and presented in the form of database files listed in Table 27. These database files are included in the archive. Figure 21 to Figure 30 of the Appendix 8.3 show the parameters currently used as sample database files.

(1) Bit depth correction

The signal in a raw image is converted to the original values at 12-bits by

$$I_1(h,v) = (I_0(h,v) + 0.5) \cdot 2^{(12-n)} \quad (1)$$

where $I_0(h,v)$ is the signal of the pixel at the image coordinate (h,v) and n is bit depth of downlinked data, either of 8, 10, or 12. The term 0.5 is added to adjust the offset caused by onboard bit depth reduction conducted by dividing image signals by $2^{(12-n)}$ on DE.

(2) Bias removal (skipped for onboard smear corrected images)

The bias of the signal is dependent on the temperatures of the CCD and the electronics of the sensor head of each camera and the temperature of the ONC-AE (ONC Analogue Electronics Control Unit, common for all camera unit).

The bias of the signal based on Tatsumi et al. (2019a) is represented by

$$I_{\mathrm{BIAS},C}(T_{\mathrm{CCD},C}, T_{\mathrm{ELE},C}, T_{\mathrm{AE}}) = \begin{cases} (320.66 + 0.652T_{\mathrm{CCD},C} - 0.953T_{\mathrm{ELE},C})(0.987 - 0.00251T_{\mathrm{AE}}), & C: \mathrm{T} \\ \sum_{k=0}^{2} a_{k,C}\, {T_{\mathrm{AE}}}^{k} \cdot T_{\mathrm{CCD},C} + \sum_{k=0}^{2} b_{k,C}\, {T_{\mathrm{AE}}}^{k}, & C: \mathrm{W1, W2} \end{cases} \quad (2)$$

where $T_{\mathrm{CCD},C}$ and $T_{\mathrm{ELE},C}$ are the temperatures of the CCD and the sensor head electronics of the camera C in degC, T_{AE} is the temperature of ONC-AE in degC, and $I_{\mathrm{BIAS},C}(T_{\mathrm{CCD},C}, T_{\mathrm{ELE},C}, T_{\mathrm{AE}})$ is the bias signal of the camera C at the condition of $(T_{\mathrm{CCD},C}, T_{\mathrm{ELE},C}, T_{\mathrm{AE}})$ in COUNT, respectively. The PDS4 attributes and keywords of these parameters are listed in Appendix 8.4. The parameters $a_{k,C}$ and $b_{k,C}$ are the coefficients of polynomial equation for W1 and W2 and their values based on Tatsumi et al. (2019a) are listed in Table 6. Then the bias correction is calculated by

$$I_2(h, v) = I_1(h, v) - I_{\mathrm{BIAS,C}}(T_{\mathrm{CCD},C}, T_{\mathrm{ELE},C}, T_{\mathrm{AE}}). \quad (3)$$

Table 6. The coefficients for bias removal for W1 and W2 (Tatsumi et al., 2019a).

C: Camera	$a_{0,C}$	$a_{1,C}$	$a_{2,C}$	$b_{0,C}$	$b_{1,C}$	$b_{2,C}$
W1	0.680	-5.74e-3	1.06e-4	260	−1.72	8.50e-3
W2	0.573	-2.95e-3	8.92e-3	288	−1.65	6.29e-3

(3) Non-linearity correction

The output signal increases mostly linearly with the input photon flux up to the signal around 3000 counts (at 12 bits). Beyond this level, the output signal starts to increase non-linearly with the input flux and finally approaches to a constant value. The exposure time is usually adjusted not to exceed the value of 3100 counts that guarantees the linearity of the signal with the input flux, however effect of non-linearity is corrected, if necessary, by

$$I_3(h, v) = I_2(h, v) \cdot \sum_{k=1}^{3} f_{k,C} I_3(h, v)^k. \quad (4)$$

The non-linearity is represented by third order polynomial equation. The coefficients of non-linearity correction for each camera C, $f_{k,C}$ are listed in Table 7. The values of Table 7 indicate that non-linea rity correction is not conducted currently, although a rough estimate is obtained in Tatsumi et al. (201 9a). These parameters will be updated in a future version, users should check the value of header key word "DYNRNGLN", which is a dynamic range of each product corresponding to 3100 counts (at 12 b its) in L2a.

Table 7. The current coefficients of non-linearity correction.

Camera	$f_{0,C}$	$f_{1,C}$	$f_{2,C}$	$f_{3,C}$
T	1	0	0	0
W1	1	0	0	0
W2	1	0	0	0

(4) Dark current correction

Dark current correction is calculated by the following equation,

$$I_4(h, v) = I_3(h, v) - t_{\mathrm{EXP}} \exp(d_{1,C} T_{\mathrm{CCD},C} + d_{0,C}), \quad (5)$$

where t_{EXP} is the exposure time in seconds and $T_{\mathrm{CCD},C}$ is CCD temperature of camera "C" in degC. Coefficients $d_{0,C}$ and $d_{1,C}$ are listed in Table 8. The values listed here are the average of the whole pixels in each CCD, although there are different dark noise trends at different pixels, which should be considered in future analysis. Standard deviation of dark current is about three time larger than the

average. The average of dark current signal is calculated to be about 0.08 count/s for the CCD temperature of −30 degC and 4.57 count/s for the CCD temperature of 10 degC.

Table 8. Coefficients for the average dark current correction.

C: camera	$d_{0,C}$ (count/s)	$d_{1,C}$ (count/s/degC)	Reference
T	0.52	0.10	Derived from in-flight calibration. Tatsumi et al. (2019a) [1].
W1	0.52	0.10	No data. Currently, ONC-T's values are used.
W2	0.52	0.10	No data. Currently, ONC-T's values are used.
Catalog	-0.164	0.114	Derived to match the catalogue value of dark current, expressed by t_{EXP} 0.849 exp(0.114 T_{ccd}) [count] as shown in Kameda et al. (2017). Preflight calibration data matches this catalogue representation.

[1] Previously dark current is expressed by 0.849τ exp(0.114 T_{ccd}) (DN) based on pre-launch calibration in Kameda et al. (2017). Current values are updated by using onboard calibration data.

(5) Smear noise reduction

The status of onboard smear correction is recognized by the FITS keyword "NSUBIMG" or the FITS keyword "SMEARCR". If NSUBIMG = 1 or SMEARCR = 'NON', the following smear noise reduction is conducted.

The equation of smear noise reduction is described by

$$I_5(h,v) = I_4(h,v) - \frac{N_v\, t_{\mathrm{VCT},C}}{N_v\, t_{\mathrm{VCT},C} + t_{\mathrm{EXP}}} \frac{\sum_{v=0}^{N_v-1} I_4(h,v)}{N_v}, \quad (6)$$

where the second term in the right hand represents smear noise for a vertical line at the horizontal position of h in the image coordinate, calculated by the same method used in Ishiguro et al. (2010), which is similar to the method of Murchie et al. (1999) and Bell et al. (2006). N_v is the number of horizontal lines (i.e., 1024 lines) and $t_{\mathrm{VCT},C}$ is the vertical charge transfer time per line in seconds for camera C. The values of $N_v\, t_{\mathrm{VCT},C}$ determined by onboard calibration are listed in Table 9.

Table 9. Coefficients for smear noise correction.

Camera	$t_{\mathrm{VCT},C}$ (μs)	$N_v\, t_{\mathrm{VCT},C}$ (ms) where $N_v = 1024$	Reference
T	7.46	7.639	Kouyama et al. (2021a)
W1	7.0	7.169	Kouyama et al. (2021a)
W2	7.2	7.373	Tatsumi et al. (2019a)

As an exception, the smear noise reduction in the ground processing is not applied to the subframe images cropped by on-board processing (ROI images described in Section 5.1.3). The reason for this is that the ground processing cannot integrate over the cropped and unacquired portion of the full-field image. However, the ROI option was often used to observe stellar-like objects in space, and smear noise of such long time exposure is negligible, so correction is not necessary.

(6) Flatfield correction

The flatfield correction is simply calculated by

$$I_6(h,v) = \frac{I_5(h,v)}{I_{\mathrm{FLAT}}(h,v)} \tag{7}$$

where $I_{\mathrm{FLAT}}(h,v)$ is the value of the normalized flatfield at the image coordinate of (h,v). $I_{\mathrm{FLAT}}(h,v)$ is created by dividing all pixel values by the average of the intensities in the central 300 × 300-pixel area.

Users should note that the flatfield depends on the temperature of CCD (Figure 11). The flatfield patterns have changed over time, once after the first touchdown (TD1) on Feb. 21, 2019, and then the second touchdown (TD2) on July 11, 2019, possibly due to dust lifted during the touchdown operations.

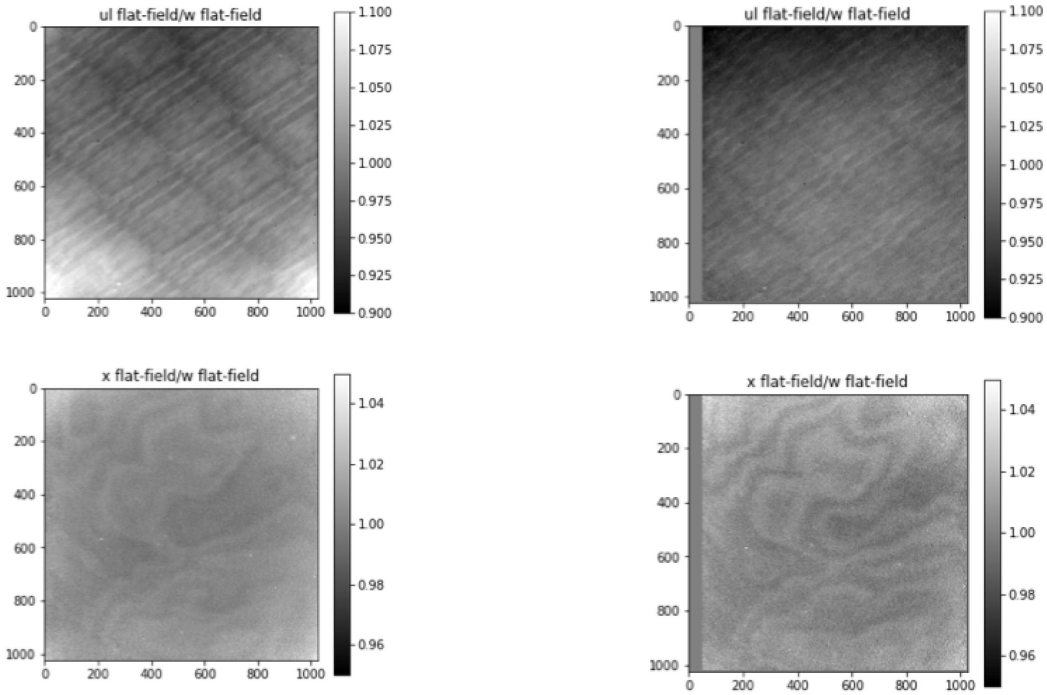

Ground calibration (room temperature) Onboard stacking (-29 degC)

Figure 11. Flatfields for ONC-T ul- and x-bands. Left is ground calibration dataset (at the room temperature) and right is created onboard at the temperature of −29 degC (from Tatsumi et al., 2019b).

Table 10 shows sets of the currently prepared flatfields. The first version of the flatfield dataset is created from ground calibration with an integrated sphere at room temperature. The second version is created by stacking the images of Ryugu acquired at the middle altitude (~3 km) during the MASCOT release operation by assuming the constant color of Ryugu's surface (October 3, 2019) at the CCD temperature of −29 degC. In this dataset, the flatfields except for v-band are trimmed because of co-registration. The third version of the flatfield set are obtained by combining the second dataset and the temperature dependence derived from FF (flatfield) lamp observation at the different CCD temperatures. To include the temperature dependence, the flatfield at a specific CCD temperature is represented by

$$I_{\mathrm{FLAT},n}\left(h,v,T_{\mathrm{ccd},C}\right) = I_{\mathrm{FLAT},n}(h,v,-29) + I'_{\mathrm{FLAT},p,n}(h,v)\left(a_n\left(T_{\mathrm{CCD},C}+29\right)\right) \tag{8}$$

where $I_{\mathrm{FLAT},n}\left(h,v,\mathrm{T}_{\mathrm{CCD},C}\right)$ is the flatfields of the band "n" at $T_{\mathrm{CCD},C}$, $I'_{\mathrm{FLAT},p,n}(h,v)$ is the temperature dependent component of the flatfields obtained by principal component analysis and a_n is the coefficient for band "n". Since only x- and p-bands have clear temperature dependence, the flatfields of the other bands are the same with the second version dataset.

Table 10. ONC flatfield dataset.

Version	Name	Applicable period	Description	Reference
1	Flatfields at room temperature	From Launch to the first touchdown	Flatfields created from on-ground calibration conducted at room temperature. Not applicable to most of the images after the launch because of temperature dependence.	Kameda et al. (2017), Suzuki et al. (2018)
2	Flatfields at the nominal CCD temperature (-29 degC) [1]	From Launch to the first touchdown	Flatfields created by stacking the images taken during MASCOT hovering (20181003) at the altitude of 3 km. CCD temperature is approximately -29 degC. During the examination among the bands, peripheral areas are trimmed.	Tatsumi et al. (2019b), Kameda et al. (2021)
3	Flatfields with CCD temperature dependence	From Launch to the first touchdown	CCD temperature dependence is considered for narrow bands of ONC-T.	Kouyama et al. (2021a)

[1] Flatfields of T-wide, W1 and W2 are same as the ground test because the images of these camera are not used for spectral studies.

Since most of the images obtained after the launch are taken at the CCD temperature ranging from −29 to −30 degC except for the two touchdowns (TD), versions 2 or 3 of the flatfield set is suitable for the most of images obtained before TD1. The version 3 was used for public release of the PDS4 data bundle. The flatfield files of this version 3 are contained in the directory 'hyb2_onc/calibration/flatfield' of the ONC PDS4 data bundle. Note that the flatfield files versions 1 and 2 of ONC-T had been only used for the internal products in the improvement process by the ONC team, and they are not included in the calibration directory of the bundle. The flatfield file names, the temperature-dependency coefficients, and the time-dependency coefficients can be found in the '.db' files contained under the directory 'hyb2_onc/calibration/database' of the bundle. Sample contents of these database files are shown in Figures 21–28 in Section 8.3. For ONC-W1 and W2, the version 3 flatfields are the same as version 1 flatfields, because it is difficult to obtain proper calibration images required to update of flatfields for ONC-W1 and W2. The peripheral areas of ONC-T narrow bands except for v-band are trimmed in the “version 2” and “version 3”. The distinction between 'full' or 'trimmed' field of view is indicated in the flatfield file names (Figure 22). The flatfield filenames for ONC-T v-band, ONC-W1 and W2 contain '_f_' to indicate a 'full' field of view. The other filenames contain '_t_' to indicate a 'trimmed' field of view.

Due to the lack of the appropriate dataset like one conducted in the MASCOT deployment operation after TD1, the creation of flatfields for images after TD1 and TD2 have not been completed yet. Therefore, the flatfields of version 3 are also applied to the data after TD1. The flatfields after TD1 are slightly different from the version 3 flatfields. Thus, users need to be careful when comparing the absolute value of I/F or reflectance for images acquired during different mission phases.

(7) Radiator stray light correction

The radiator stray light contamination is caused by the reflection of sunlight by a part of ONC-T radiator which was first reported in Suzuki et al. (2018). The radiator stray light was monitored intensively onboard during the cruise phase. The intensity and pattern of the stray light was found to be strongly dependent on the spacecraft attitude with respect to the Sun (Tatsumi et al., 2019a). The spacecraft attitude can be expressed by two parameters φ and γ, which are the angle between

Hayabusa2-Sun vector and Z_{SC} and the twisting angle around Z_{SC}. It has been found that the stray light is negligible (< 3.8 count/s at 1 AU) when $\varphi < -7^\circ$ or $\gamma > -10^\circ$. Thus, the observations were conducted in this condition as much as possible. However, the strict operation conditions sometime did not allow us to observe Ryugu in the weak stray light condition, for example MASCOT and MINERVA-II deployments, touchdowns, and their rehearsals. In these cases, we applied the radiator stray light removal based on the model derived in Tatsumi et al. (2019a). The modeled stray light image can be given by $I_{\mathrm{sl}} = i_{\mathrm{sl}} M_{\mathrm{sl}}$, where i_{sl} is the intensity of stray light and M_{sl} is the stray light pattern in the FOV. Both of them can be expressed as functions of the spacecraft attitude.

$$i_{\mathrm{sl}} = (-0.0879\varphi^3 - 5.61\varphi^2 - 119.4\varphi - 603.8)(-0.0037\gamma^2 + 0.113\gamma + 0.956), \quad (9)$$

$$M_{\mathrm{sl}} = M_{\mathrm{ave}} + (0.02105\varphi^2 + 1.338\varphi + 17.02)M_{\mathrm{PC1}}, \quad (10)$$

where M_{ave} and M_{PC1} were derived from the principal component analysis of stray light images with various spacecraft attitudes. Thus, the stray light can be removed as

$$I_7 = \begin{cases} I_6, & \varphi < -7^\circ \text{ or } \gamma > -10^\circ \\ I_6 - \frac{I_{sl}\, t_{\mathrm{EXP}}}{{R_{\mathrm{sol}}}^2}, & \text{otherwise} \end{cases}, \quad (11)$$

where t_{EXP} is the exposure time in seconds and R_{sol} is the solar distance in AU. Note that the radiator stray light was assessed the attitude of $\gamma > -30^\circ$, meaning that this model cannot be applied for the images taken $\gamma < -30^\circ$.

5.3.2.3 Level 2c – Distortion Corrected and Physically Converted Image Data

Offset of a center of field of view (FOV) and image distortion of a raw image are corrected by using the functions obtained by onboard star field observation (Suzuki et al., 2018). The magnitude of the distortion is expressed as a polynomial function of distance from the position of the optical axis (assumed to be the same as the center of the FOV) in the image coordinates. The distortion is corrected using the functions described in the following section. After conducting the distortion correction, the image is normalized by the exposure time to represent signal in count/s at a given CCD temperature. Then the digital signal is multiplied by the conversion factor at a given CCD temperature to obtain radiance represented in physical units of spectral radiance (W/m^2/μm/str). The conversion factors are included in the database file prepared for calibration, hyb2_onc_c_radc_yyyymmdd.db (see 6.2.10.3).

The final level 2c (L2c) image data is a FITS file with two HDUs containing header metadata and a calibrated image data of main detector area (1024 pixels × 1024 pixels). The data is represented in spectral radiance (W/m^2/μm/str).

The details of the processing are as follows:

(1) Distortion correction

Distortion of the ONC images is represented as the function of the distance of the pixel (h, v) from the optical axis in the image coordinates (Suzuki et al., 2018). The position of the optical axis is defined as the center of FOV and calculated by

$$\begin{pmatrix} h_{\mathrm{c}} \\ v_{\mathrm{c}} \end{pmatrix} = \begin{pmatrix} (N_{\mathrm{h}} - 1)/2 \\ (N_{\mathrm{v}} - 1)/2 \end{pmatrix}, \quad (12)$$

where $(h_{\mathrm{c}}, v_{\mathrm{c}})$ is the center of FOV, N_{h} and N_{v} are 1024, the number of lines and samples of the raw image. Then the distance r of the pixel (h, v) from the optical axis is calculated by

$$r = \sqrt{(h - h_{\mathrm{c}})^2 + (v - v_{\mathrm{c}})^2}\ . \quad (13)$$

Given the point source at a distance r is projected to a point at a distance r' in the same direction from the optical axis due to distortion, Suzuki et al. (2018) obtained the relationship between r and r' of ONC cameras by

$$r' = \mathrm{dist}(r) = r + \varepsilon_1 r^3 + \varepsilon_2 r^5 \ , \tag{14}$$

where ε_1 and ε_2 are the distortion parameters. The obtained values of ε_1 and ε_2 are summarized in Table 11 with their RMS errors for fitting.

Table 11. Distortion function data (based on Suzuki et al., 2018).

	ε1	ε2	RMS error (pixel)
T	-9.28e-9	0	0.16
W1	3.134e-7	-1.716e-13	0.6
W2	2.893e-7	-1.365e-13	0.5

The creation of distortion corrected image is conducted by re-sampling with the use of equation (14). The re-projection of the point in the undistorted image to distorted image is represented by

$$\begin{pmatrix} h \\ v \end{pmatrix} = \frac{\mathrm{dist}^{-1}(r')}{r'} \begin{pmatrix} h' - h_c \\ v' - v_c \end{pmatrix} + \begin{pmatrix} h_c \\ v_c \end{pmatrix} , \tag{15}$$

where (h', v') is the position of the point in the undistorted (distortion corrected) image, (h, v) is the corresponding point of in the distorted image and $r' = \sqrt{(h' - h_c)^2 + (v' - v_c)^2}$. The intensity at (h', v') in the undistorted image is estimated from the intensities of grid points nearby the corresponding point (h, v) in the distorted image by bi-linear interpolation as

$$\begin{aligned} I_8(h', v') = {} & (1 - dh)(1 - dv) I_7(h_0, v_0) \ + dh(1 - dv) I_7(h_0 + 1, v_0) \\ & + (1 - dh) dv \, I_7(h_0, v_0 + 1) \ + dh \, dv \, I_7(h_0 + 1, v_0 + 1) \ , \end{aligned} \tag{16}$$

where $h_0 = \mathrm{int}(h), v_0 = \mathrm{int}(v), dh = h - h_0$, and $dv = v - v_0$.

The inverse function $\mathrm{dist}^{-1}(r')$ in equation (15) is analytically obtained by using Cardano's equation when $\varepsilon_2 = 0$, which is described by

$$r = \mathrm{dist}^{-1}(r') = \frac{2}{\sqrt{-3\varepsilon_1}} \cos\left(\frac{1}{3}\alpha - \frac{2}{3}\pi\right) , \tag{17}$$

where

$$\alpha = \cos^{-1} \frac{r'}{2\epsilon_1 \sqrt{1/(-27{\epsilon_1}^3)}} \ . \tag{18}$$

We use this equation for ONC-T distortion correction. Since the equation is not applicable to ONC-W1 and ONC-W2, $\mathrm{dist}^{-1}(r')$ for ONC-W1 and ONC-W2 are approximated by a 5-th order polynomial functions represented by

$$r = \mathrm{dist}^{-1}(r') = r' + \sum_{k=1}^{5} c_{k,C} \ r'^k \ . \tag{19}$$

The values of coefficients $c_{k,C}$ for ONC-W1 and ONC-W2 are summarized in Table 12.

Table 12. Distortion function (inverse function) parameter in equation (19).

Coefficient	c_1	c_2	c_3	c_4	c_5
W1	9.99570e-1	1.19590e-5	-4.15730e-7	3.71770e-10	-9.07150e-14
W2	9.99340e-1	1.42190e-5	-3.93550e-7	3.41040e-10	-8.54530e-14

(2) Alignment offset correction

Table 13 summarizes the alignment offset between the spacecraft coordinates and the ONC camera coordinates obtained by the analysis of star field images (Tatsumi et. al., 2019a). Note that the alignment offset correction is not conducted in the pipeline process, because this effect is considered in creation of backplanes described in Section 6.2.6. If users are willing to correct alignment offset at the same time with distortion correction, equation (15) should be replaced by

$$\begin{pmatrix} h \\ v \end{pmatrix} = \frac{\mathrm{dist}^{-1}(r')}{r'} \begin{pmatrix} h' - h_c \\ v' - v_c \end{pmatrix} + \begin{pmatrix} h_c + h_{\mathrm{offset}} \\ v_c + v_{\mathrm{offset}} \end{pmatrix} \tag{20}$$

where $(h_{\mathrm{offset}}, v_{\mathrm{offset}})$ is the alignment offset.

Table 13. Alignment offset (Tatsumi et al., 2019a).

Camera	h_{offset} (pixel)	v_{offset} (pixel)
T	9.5	-22.5
W1	-3.5	-2.5
W2	0.5	-0.5

(3) Conversion to the radiance

Signals $I_8(h, v)$ in COUNT are then converted into radiance in unit of W/m^2/μm/str. The sensitivity of each camera or band is known to have dependence on the CCD temperature. In particular, the sensitivity of each band of ONC-T is found to have been decreased linearly with time after the TD2 (Kouyama et al., 2021a). Thus, the sensitivities of the specific band at a specific time in a specific period is given by

$$S_{n,p}(T_{\mathrm{CCD},C}, t_p) = S_{0,n,p}(1 + S'_{n,p} t_p)(a_{\mathrm{CCD},n}(T_{\mathrm{CCD},C} + 30\ \mathrm{degC}) + 1)\,, \tag{21}$$

where $S_{n,p}(T_{\mathrm{CCD},C}, t_p)$ is the sensitivity in the period "p" and the band "n", t_p is time from the start of the period in day, $S_{0,n,p}$ is the sensitivity of a specific band "n" at the start time of the period at the $T_{\mathrm{CCD},C} = -30$ degC in (count/s)/(W/m^2/μm/str). $S'_{n,p}$ is the degradation rate of the sensitivity in (day^{-1}), $a_{\mathrm{CCD},n}$ is the coefficient of the sensitivity dependence on $T_{\mathrm{CCD},C}$ for the band "n". Finally, the signal is converted to the spectral radiance by

$$I_9(h, v) = \frac{I_8(h,\ v)}{t_{\mathrm{EXP}} S_{n,p}(T_{\mathrm{CCD},C}, t_p)}\ . \tag{22}$$

The parameter values of $S_{0,n,p}$, $S'_{n,p}$, $a_{\mathrm{CCD},n}$ obtained based on star observation and described in Kouyama et al. (2021a) are listed in Table 14. The time-dependent sensitivity coefficients $S'_{n,p}$ only apply to images acquired after TD2, while for the first two time periods before TD1 and between TD1 and TD2, constant sensitivity coefficients as listed in Table 14. In addition, please note the sensitivities of the p-filter is corrected to match the lunar observation because there was a large difference between the lunar observation and the estimates of the sensitivities based on inflight star observation.

Table 14. The sensitivity of each band at $T_{\mathrm{CCD},C}$ of −30 degC (Tatsumi et al., 2019a and Kouyama et al., 2021a). These values are obtained by star observation except for the p-filter, for which we use the value based on the lunar observations (see Tatsumi et al., 2019a).

Camera: bands	$S_{0,n,p}$ Sensitivity at $T_{\mathrm{CCD},C}$ = −30 degC (count/s)/(W/m^2/μm/str)			$S'_{n,p}$ (day^{-1})	$a_{\mathrm{CCD},n}$
	1: Before TD1	2: Between TD1 and TD2	3: After TD2	3: After TD2	All
T: ul	439.1 ± 2.2	410.1 ± 11.6	399.7 ± 10.8	−0.000252	−0.001449 ± 0.00244
T: b	969.3 ± 7.9	899.1 ± 22.2	879.6 ± 22.1		−0.000968 ± 0.00108
T: v	1175.0 ± 10.0	1092.8 ± 25.5	1071.2 ± 25		−0.000814 ± 0.00090
T: Na	546.9 ± 2.0	510.9 ± 12.2	498.3 ± 11.9		−0.000866 ± 0.00154
T: w	1515.0 ± 19.3	1418.9 ± 35.1	1380.5 ± 34		−0.000355 ± 0.000112
T: x	1499.8 ± 24.6	1405.8 ± 40.7	1373.5 ± 37.4		0.001771 ± 0.000158
T: p	961.2 ± 28.8	898.9 ± 39.8	882.6 ± 38.9		0.004201 ± 0.000202
T: wide	18412	17124	16786	−0.000252	−0.000814[1]
W1	1.38×10^3	$5.2\times10^2 \pm 0.8\times10^2$	$5.0\times10^2 \pm 0.8\times10^2$	0	−0.000814[1]
W2	3.84×10^3	3.84×10^3	3.84×10^3	0	−0.000814[1]

[1] The values are not determined. The estimate for v-band is used instead as the representative value.

5.3.2.4 Level 2d – Derived I/F Image Data

The I/F data product is produced by dividing the L2c images with the effective solar irradiance for each band. The effect of solar distance is adjusted using the solar distance value calculated by using the spacecraft ephemeris, spacecraft orbit and time stamp that are stored in the level 2a data product header.

The final level 2d (L2d) image data is a FITS file with two HDUs containing header metadata and I/F data of the main area (1024 pixels × 1024 pixels).

The I/F data is calculated by following equation,

$$\mathrm{I/F} = I_{10}(h,v) = \frac{I_9(h,v)\,\pi\,{R_{\mathrm{sol}}}^2}{I_{\mathrm{sol},n}}, \tag{23}$$

where $I_{\mathrm{sol},n}$ is the effective solar irradiance (W/m^2/μm) of the specified band (or camera) "n" for the Sun at 1 AU. Table 15 shows the values of $I_{\mathrm{sol},n}$ used in the pipeline (Tatsumi et al., 2019a) together with effective band center and band width for solar spectrum.

Table 15. The estimated effective solar irradiance for each band or camera (Tatsumi et al., 2019a). The band center and the band width are effective values calculated for solar spectrum and the system efficiency of each camera or band.

Camera: Band	Effective band center λ_c [nm]	Effective band width $\Delta\lambda_{band}$ [nm]	Effective solar irradiance (W/m^2/μm) $I_{sol,n}$	Reference
T: ul	397.5	34.7	1343.7	Tatsumi et al. (2019a)
T: b	479.8	26.7	1969.1	
T: v	548.9	27.9	1859.7	
T: Na	589.9	11.6	1788.0	
T: w	700.1	28.8	1414.4	
T: x	857.3	42.4	985.8	
T: p	945.1	57.2	834.9	
T: wide	612[1]	448 [1]	1455.1 [1]	The values are calculated with Eqs. (3.1) and (3.2) in Tatsumi et al. (2019a).
W1	575	145	1784.5	
W2	567	150	1798.4	

[1] These properties listed in Kouyama et al. (2021a) are replaced with the values obtained by the same method for W1 and W2 in this document after examination.

5.3.2.5 Level 2e - Derived Photometrically Corrected Reflectance Image Data

The reflectance data product is produced from the I/F data by applying the photometric correction. Photometric function modeled by Hapke (1981; 1984; 2012) and the viewing geometry are used for the conversion. The viewing geometry is a set of incidence angle i, emission angle e, and phase angle α that are calculated for each pixel by providing a shape model, ephemeris, spacecraft orbit, attitude, and imaging time.

The final level 2e (L2e) image data is a FITS file with two HDUs containing header metadata and reflectance factor data of main area (1024 pixels × 1024 pixels).

The reflectance factor (REFF) is defined as the ratio of the reflected light intensities from a target and a reference surface (a perfect diffuse surface) under the same observation geometry (Hapke 2012). Since many laboratory reflectance measurements of the meteorite samples have been presented in this definition at the phase angle of 30°, we also choose this value as the level 2e output.

Based on a modeled photometric function in Hapke (1981; 1984; 2012), hereafter Hapke's model, the radiance factor (RADF or I/F) for the observation condition (i, e, α) at wavelength λ, $\mathrm{RADF}(i, e, \alpha, \lambda)$, is given by

$$\mathrm{RADF}(i, e, \alpha, \lambda) = \frac{w}{4}\frac{\mu_{0e}}{\mu_{0e} + \mu_e}\{[1 + B(\alpha)]p(\alpha) + H(\mu_{0e})H(\mu_e) - 1\}S(i, e, \alpha, \bar{\theta}). \quad (24)$$

The mathematical derivation of these terms can be found in Hapke (2012). Although the mathematical expression of these terms is long, we list them bellow for clarification.

The parameter w is single scattering albedo. The opposition effect term, $B(\alpha)$, is expressed as

$$B(\alpha) = \frac{B_0}{1 + \frac{\tan(\alpha/2)}{h}}, \quad (25)$$

where B_0 and h are the parameters about the strength and width of opposition effect, respectively. For the phase function $p(\alpha)$, we employed 1-parameter Henyey-Greenstein function as

$$p(\alpha) = \frac{(1-g^2)}{[1+2g\cos(\alpha)+g^2]^{3/2}}, \tag{26}$$

where g is a parameter to describe the phase curve. Note that the photometry researchers also use another definition of $+/-$ signs in the denominator of Henyey-Greenstein function, however, this difference can be absorbed by reversing the positive and negative definitions of the parameter (note that the definition of g is different from one in Tatsumi et al., 2020).

The $H(y)$ terms are the Chandrasekhar H-functions to describe multiple scattering, which are estimated using the expression

$$H(y) = \frac{1+2y}{1+2y\sqrt{1-w}}. \tag{27}$$

The surface roughness term, $S(i,e,\alpha,\bar{\theta})$, accounts for the largescale roughness parameter $\bar{\theta}$ [deg], and μ_{0e} and μ_e are the modified cosines of the incident and emission angles, respectively, due to roughness. Expressions of $S(i,e,\alpha,\bar{\theta})$, μ_{0e} and μ_e vary depending on the relationship of i and e.

When $i \le e$,

$$S(i,e,\psi) = \frac{\mu_e}{\eta(e)}\frac{\cos(i)}{\eta(i)}\frac{\chi(\bar{\theta})}{1-f(\psi)+f(\psi)\chi(\bar{\theta})[\cos(i)/\eta(i)]}, \tag{28}$$

$$\mu_{0e} = \chi(\bar{\theta})\left[\cos(i)+\sin(i)\tan(\bar{\theta})\frac{\cos(\psi)\,E_2(e)+\sin^2(\psi/2)\,E_2(i)}{2-E_1(e)-(\psi/\pi)E_1(i)}\right], \tag{29}$$

$$\mu_e = \chi(\bar{\theta})\left[\cos(e)+\sin(e)\tan(\bar{\theta})\frac{E_2(e)-\sin^2(\psi/2)\,E_2(i)}{2-E_1(e)-(\psi/\pi)E_1(i)}\right], \tag{30}$$

otherwise ($e < i$)

$$S(i,e,\psi) = \frac{\mu_e}{\eta(e)}\frac{\cos(i)}{\eta(i)}\frac{\chi(\bar{\theta})}{1-f(\psi)+f(\psi)\chi(\bar{\theta})[\cos(e)/\eta(e)]}, \tag{31}$$

$$\mu_{0e} = \chi(\bar{\theta})\left[\cos(i)+\sin(i)\tan(\bar{\theta})\frac{E_2(i)+\sin^2(\psi/2)\,E_2(e)}{2-E_1(i)-(\psi/\pi)E_1(e)}\right], \tag{32}$$

$$\mu_e = \chi(\bar{\theta})\left[\cos(e)+\sin(e)\tan(\bar{\theta})\frac{\cos(\psi)\,E_2(i)+\sin^2(\psi/2)\,E_2(e)}{2-E_1(i)-(\psi/\pi)E_1(e)}\right], \tag{33}$$

where $\chi(\bar{\theta})$, $\eta(y)$, $E_1(y)$, $E_2(y)$, $f(\psi)$, and the azimuth angle ψ are defined by

$$\chi(\bar{\theta}) = 1/[1+\pi\tan^2(\bar{\theta})]^{1/2}, \tag{34}$$

$$\eta(y) = \chi(\bar{\theta})\left[\cos(y)+\sin(y)\tan(\bar{\theta})\frac{E_2(y)}{2-E_1(y)}\right], \tag{35}$$

$$E_1(y) = \exp\left[-\frac{2}{\pi}\cot(\bar{\theta})\cot(y)\right], \tag{36}$$

$$E_2(y) = \exp\left[-\frac{1}{\pi}\cot^2(\bar{\theta})\cot^2(y)\right], \tag{37}$$

$$f(\psi) = \exp\left[-2\tan\left(\frac{\psi}{2}\right)\right], \tag{38}$$

$$\psi = \arccos\left[\frac{\cos(\alpha) - \cos(e)\cos(i)}{\sin(e)\sin(i)}\right], \tag{39}$$

respectively.

The I/F of Level 2d product, $I_{10}(h, v)$, is converted into reflectance factor REFF at the standard viewing geometry $(i, e, \alpha, \lambda) = (30°, 0°, 30°, \lambda)$ which can be compared with laboratory measurement by the following equation:

$$\mathrm{REFF}(h, v) = I_{11}(h, v) = \frac{I_{10}(h, v)\ \mathrm{RADF}(30°, 0°, 30°, \lambda)}{\mathrm{RADF}(i, e, \alpha, \lambda)\cos(30°)}\ . \tag{40}$$

Parameters of Hapke's model for each band used in equation (24) to (39) are determined in Tatsumi et al. (2020) and summarized in Table 16.

Table 16. Hapke parameter for Ryugu (based on Tatsumi et al., 2020).

Camera: band	w	g [1]	B_0	h	$\bar{\theta}$	Reference
T: ul	0.047 ± 0.008	-0.386 ± 0.001	0.98 ± 0.021	0.075 ± 0.008	28° ± 6°	Tatsumi et al. (2020)
T: b	0.045 ± 0.008	-0.388 ± 0.001				
T: v	0.044 ± 0.008	-0.388 ± 0.001				
T: Na	0.044 ± 0.008	-0.387 ± 0.001				
T: w	0.045 ± 0.008	-0.382 ± 0.001				
T: x	0.047 ± 0.008	-0.374 ± 0.001				
T: p	0.046 ± 0.008	-0.377 ± 0.001				
T: wide	0.044 ± 0.008	-0.388 ± 0.001	0.98 ± 0.021	0.075 ± 0.008	28° ± 6°	Not determined yet. Parameters for T: v is used instead.
W1						
W2						

[1] The definition of g is different from one in Tatsumi et al. (2020) and their values are adjusted to be consistent with the definition in this document.

5.3.2.6 Level 2dbpc – Derived Backplane Cube Data

Backplane data provides ancillary information that includes longitude, latitude, viewing geometry parameters (incidence angle, emission angle, solar phase angle), plate ID, and distance between the spacecraft and asteroid surface. The backplane data is calculated for each L2d product and provided in a FITS-cube format. This data is created by using the software "plate_renderer" (Hirata, 2018) by entering SPICE kernels of spacecraft trajectories, attitude, and asteroid shape. Output files of plate_renderer were converted to a single FITS file with the 3-dimensional data array. The FITS keywords in the FITS file were extracted from L2d product after creation of corresponding L2d product. Backplane data file is not included in the archive if there is no asteroid in the image or SPICE kernels are not available to calculate geometry at time of image acquisition.

5.3.2.7 Level 2drc – Derived Co-Registered I/F Image Cube Data

Co-Registered I/F Cube Image Data includes the spatially aligned multi-band image dataset or consecutively shot single band image dataset.

Since ONC-T utilizes a filter wheel device for obtaining multi-band images, positions of Ryugu surface features in a certain band image of ONC-T are slightly different from the other bands

because of the rotation of Ryugu and variation of spacecraft position and attitude. To investigate the surface spectrum of Ryugu from ONC-T multi-band images, accurate image registration is essential to avoid an error caused from mis-registration. To achieve the accurate image registration (i.e., sub-pixel level image registration), an image registration technique that repeats template matching and affine transformation three times with a coarse-to-fine approach (Tanimoto and Pavlidis, 1975; Rosenfeld and Vanderbrug, 1977) is adopted. This co-registration process is also required to utilize consecutively shot single band images.

Figure 12 shows the calculation flow of the coarse-to-fine approach used in the ONC-T image registration. The detail of this method is described in Kouyama et al. (2021b) and summarized in (1) of this section.

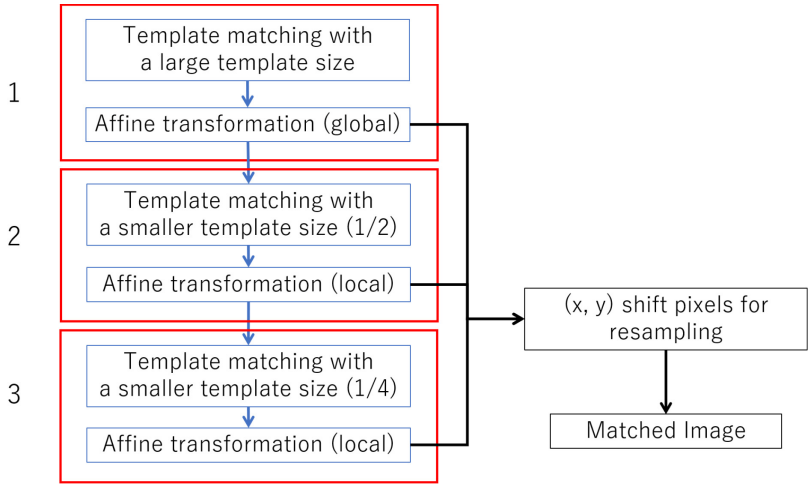

Figure 12. Calculation flow of image registration for ONC-T multi-band images in ONC-T pipeline.

During co-registration, master band image (or reference band image) was determined for each multi-band observation. In the ONC-T pipeline, a band taken in the middle of image sequence is defined as a reference band. Table 17 shows temporal imaging order and the master band defined.

Table 17. Temporal image sequence and master band for co-registration.

Number of bands in image sequence	Temporal order of filters in image sequence	master band image
3	v, ul, x	ul
4	v, ul, b, x	ul
	v, w, x, ul [1]	x
6	v, w, x, p, b, ul	x
7 (nominal)	v, w, x, Na, p, b, ul	Na
Up to 32 (consecutively shot single band image)	Single band	middle of temporal sequence

[1] This band set is used only for the date of 2019-02-07.

The total number of frames can be checked with the FITS header keyword NAXIS3. The wavelength of each frame can be checked with the FITS header keyword FILTERxx. The browsing JPEG images of l2drc have a margin below the image to indicate the bands included in the cube and the bands used in that pseudo-color RGB.

Some special l2drc files, consecutively shot single band have 32 frames in them. These data exist for the following five observation dates: 2018-11-13, 2019-02-05, 2019-02-07, 2019-06-05, and 2019-06-07. The special observations (8-consecutive shots in one band × 4-bands) were made on these dates to reduce noise by stacking. As a result, 32 images for one rotational phase of the asteroid were obtained. In the image co-registration process, the 15th frame was used as reference frame. The user of these cubes can obtain an I/F with reduced noise by performing some statistical processing on 8 images per band. The simplest method is to average the 8 frames, but the method is left to the user.

(1) Image registration procedure

Template matching is conducted to obtain so called optical flow vectors in two different band images as illustrated in Figure 13. At the first image registration step, which is for coarse matching, a template size of 129 × 129 pixels is used, and templates are set with an interval of 64 pixels in both x and y directions. For the second and third steps, half and 1/4 size templates are used with shorter (half and 1/4) intervals, respectively. The template matching is performed based on cross correlation between a template and a search area, and a sub-pixel estimation of finding a matched position is adopted that is based on a method described in Ogohara et al. (2012). Next, affine transformation is conducted for adjusting an image of a target band to an image of a reference band based on the optical flow vectors.

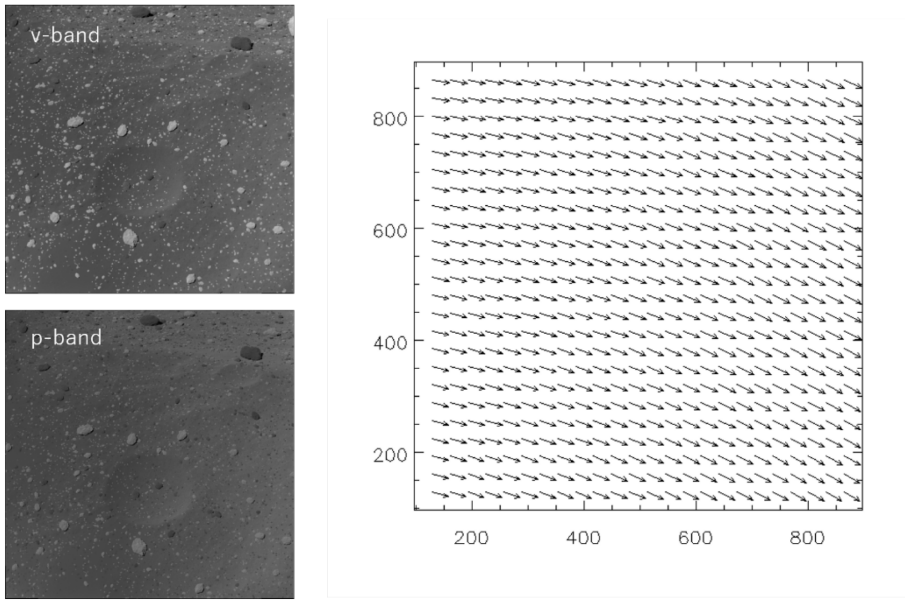

Figure 13. An example of optical flow vectors obtained from v-band (a reference band) and p-band (a target band) images.

The difference of Ryugu surface between two images is expected to be large at the first step, thus one affine matrix that is derived from whole optical flow vectors is used for the affine transformation of all pixels. Then, local affine transformation is conducted at every position of optical flow vector at the second and third steps, because non-uniform transformation is required for matching two band images with a sub pixel level due to the complicated Ryugu surface shape. In the local affine transformation, only 9 vectors (a vector at a target template position and 8 surrounding vectors) are used for estimating a local affine matrix and an affine transformation is conducted within a region in the target template. Note that measured shift pixels in x and y directions for matching images are also stored at every affine transformation step (Figure 14).

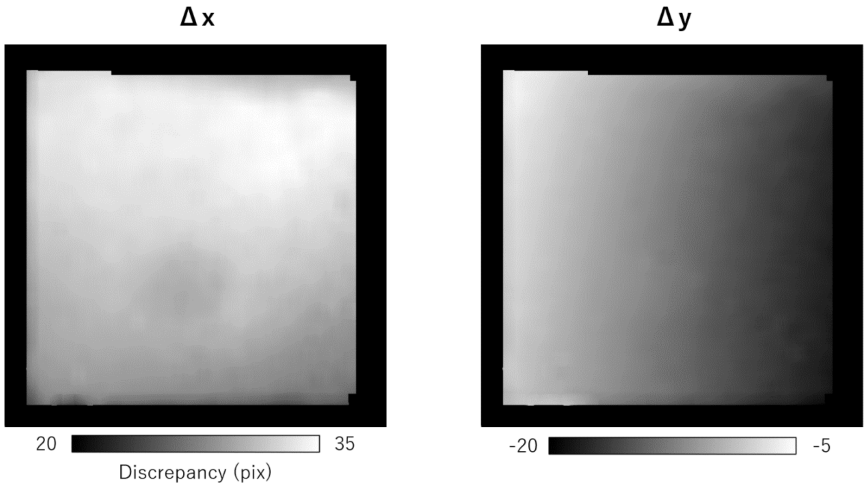

Figure 14. An example of measured pixels for shifting an image for image registration.

Finally, the "original" target image is adjusted to the reference image with a bilinear interpolation by using the obtained x and y shift pixels after three affine transformations. This procedure aims to perform resampling only once and thus to avoid image blurring due to the resampling as much as possible.

It should be noted that a feature-based matching technique (e.g., SURF) is adopted before conducting the coarse-to-fine approach of the image registration when applied to low-altitude images. For low-altitude images, the distance of the same feature in the two images may be half of the ONC-T image frame. Computation time is excessive if the template matching technique is used with a large search area.

(1) Example and accuracy of image registration

As an example, the image registration was adopted to multi-band Earth images that were obtained after the Hayabusa2 Earth swing-by operation. Because the position and attitude of Hayabusa2 gradually varied during an imaging sequence, Earth positions in different band images were slightly different. Due to this slight difference, an image of band ratio (e.g., w-band and x-band image pair used for vegetation evaluation) appeared to be a shape enhanced image (Figure 15a). On the other hand, after performing the image registration, shapes of continents of the Earth are more natural (Figure 15b).

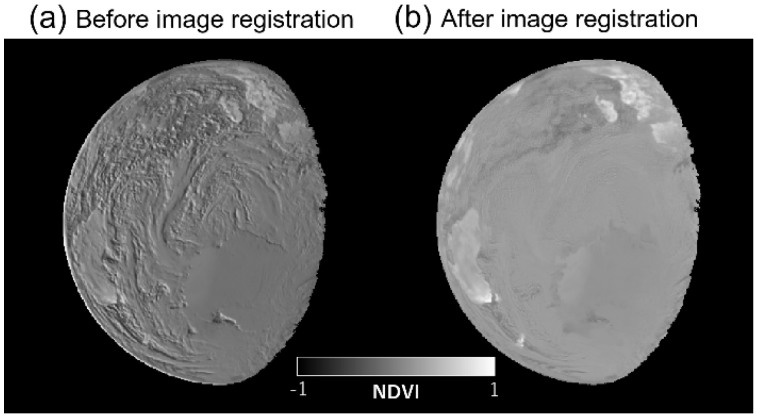

Figure 15. Normalized Difference Vegetation Index (NDVI) measured from Earth images taken by ONC-T (R: w-band, IR: x-band, NDVI $= (\mathrm{IR} - \mathrm{R})/(\mathrm{IR} + \mathrm{R})$), (a) before and (b) after applying image registration procedure.

To evaluate the accuracy of the image registration, we shifted an Earth image with sub-pixel values in both x and y directions artificially, and then by applying the image registration with the original image and the shifted image. In x direction, we simply shifted the image with 0.5 pixel. In y direction, we shifted the image with $\sin(y/256 \times 2\pi)$ pixels to evaluate possible local motions. Figure 16 shows the magnitude of pixel shifting measured by the image registration. We confirmed that the mean shift value in x direction was 0.5 ± 0.08 pixel, indicating that our method can match images at a sub-pixel level. Similar performance was also confirmed in y direction.

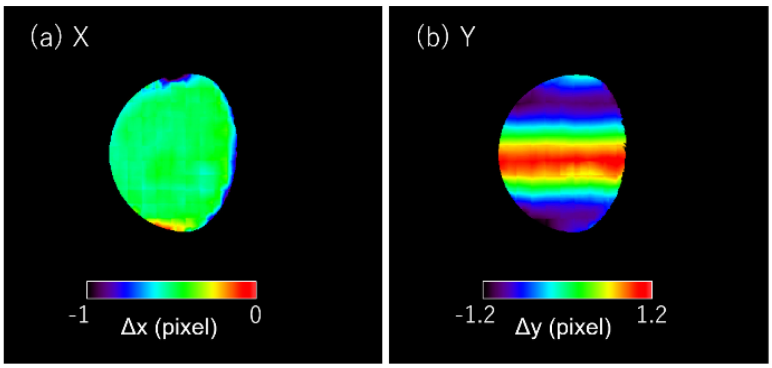

Figure 16. Derived displacement pixels in (a) x and (b) y directions using an artificially shifted Earth image. The given displacements were 0.5 pixel in x direction and $\sin(y/256 \times 2\pi)$ in y direction, respectively.

5.3.2.8 Level 2erc – Derived Co-Registered Photometrically Corrected Reflectance Image Cube Data

Level 2erc (L2erc) images are also spatially aligned using the same method used for L2drc, but for L2e reflectance images. L2e images are generally noisy because of mismatch of local morphology. Identifying similar features in L2e images is difficult so L2d images are used to determine the shift of the identical points among the bands of L2e.

5.3.3 Data Flow

ONC raw, calibrated, and derived data products are built up in sequential data processing steps addressing specific corrections or calibrations. All data products are built from raw telemetry ingested into the SIRIUS database. The ONC data processing pipelines query the database directly for new raw science data. The ONC data files generated by the pipelines are returned for storage. Figure 17 shows the ONC data flow from raw telemetry to derived data products. Note that only L2a products are created for optical images and only L2a and L2b products are created for 0-sec exposure images obtained for the purpose of bias check. L2drc, L2e, and L2erc are created for images in the approach phase, the asteroid proximity phase, and the return phase.

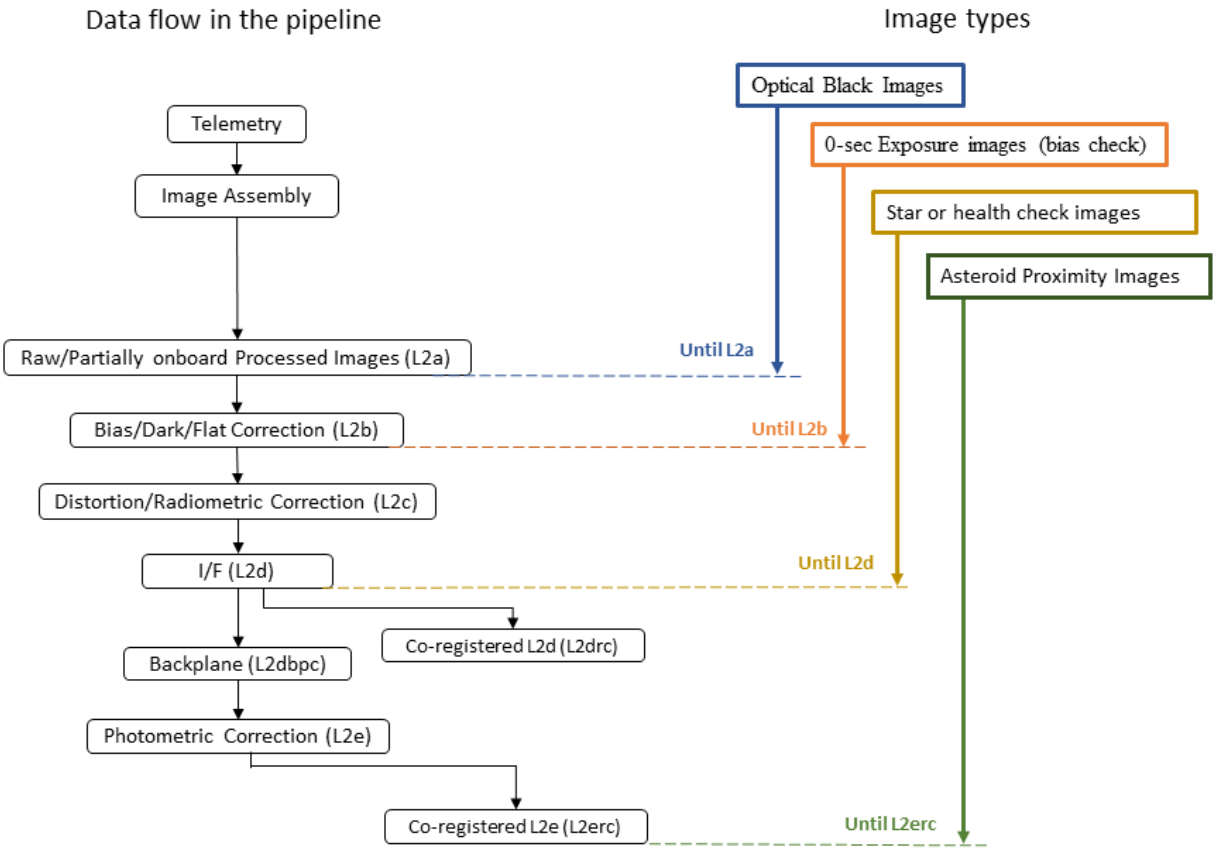

Figure 17. ONC data processing flow diagram for each type of images.

Table 18 shows the expected ONC science data collection for each mission phase. The data volume of the processed data products. Derived data products are produced once time over the course of the mission.

Table 18. Data Volume by Mission Phase

Mission Phase	Commissioning	EDVEGA	Earth Swing-by	Transfer	Approach	Asteroid Proximity	Return	Reentry	Total
L2a: Raw	179 MiB	182 MiB	1.2 GiB	3.4 GiB	2.1 GiB	31 GiB	1.0 GiB	-	**39 GiB**
L2b: Partially Processed	320 MiB	337 MiB	2.2 GiB	6.0 GiB	3.9 GiB	57 GiB	1.9 GiB	-	**71 GiB**
L2c: Calibrated	223 MiB	326 MiB	2.1 GiB	4.8 GiB	3.8 GiB	56 GiB	1.9 GiB	-	**69 GiB**
L2d: I/F	223 MiB	326 MiB	2.1 GiB	4.8 GiB	3.8 GiB	56 GiB	1.9 GiB	-	**68 GiB**
L2e: Photometrically Corrected	-	-	-	-	691 MiB	2.8 GiB	-	-	**3.4 GiB**
L2drc: co-registered L2d	-	-	-	-	-	24 GiB	-	-	**25 GiB**
L2erc: co-registered L2e	-	-	-	-	-	1.1 GiB	-	-	**1.1 GiB**
L2dbpc: geometry	-	-	-	-	4.5GiB	319 GiB	11 GiB	-	**334 GiB**

5.3.4 Labeling and Identification

All ONC data products are labeled with PDS4 compliant detached XML labels. These labels describe the content and format of the associated data product. Labels and products are associated by

file name with the label having the same name as the data product except that the label file has an .xml extension.

Labels are constructed with the PDS4 Product Class, Product_Observational sub-class. The Product_Observational sub-class describes a set of information objects produced by an observing system. A hierarchical description of the contents of Product_Observational products appears below:

Product_Observational
- **Identification_Area** – attributes that identify and name an object
  - logical_identifier – a unique identifier urn:jaxa:darts:hyb2_tir:<collection>:<file_name_root>, e.g., urn:jaxa:darts:hyb2_onc:data_raw:hyb2_onc_20181025_022350_tvf_l2a
  - version_id – version of product
  - title – Short description of product used as the PDS4 search return
  - information_model_version – version of PDS4 information model used to create product
  - product_class – attribute provides the name of the product class (Product_Observational)
- **Observation_Area** – attributes that provide information about the circumstances under which the data were collected.
  - Time_Coordinates – time attributes of data product
  - Primary_Results_Summary – high-level description of the types of products included in the collection or bundle
  - Investigation_Area – mission, observing campaign or other coordinated, large-scale data collection attributes
  - Observing_System – observing system (instrument) attributes
  - Target_Identification – observation target attributes
  - Mission_Area – mission specific attributes needed to describe data product
  - Discipline_Area – discipline specific attributes needed to describe data product
- **File_Area_Observational** – describes a file and one or more tagged_data_objects contained within.
  - File – identifies the file that contains one or more data objects
  - Header – defines a header of HDU of FITS file
  - Array_2D_Image – defines a 2D image array

Information in the preceding paragraphs was distilled from the PDS4 Information Model provided by PDS. Additional information on product labels can be found at https://pds.nasa.gov/datastandards/about/.

ONC data products for l2a, l2b, l2c, l2d, l2e, l2drc, l2erc, and l2dbpc are identified with file names in the format of:

hyb2_onc_*yymmdd_hhmmss_CBA_level*.{fit, xml}

The definition of symbols is described in Table 19.

Table 19. Definition of ONC L2a, L2b, L2c, L2d, L2e, L2drc, L2erc, and L2dbpc filename

Symbol	Contents
yyyymmdd_hhmmss	Median time between the start and end times of imaging. This date is derived from the values of FITS keyword "DATE-OBS".
CBA	Camera type, band for ONC-T, and image area *A* ▪ *CB* (camera and band): w1, w2, t*F* ▪ *F* (filter or bands): u: ul-band, i: wide, v: v-band, w: w-band, x: x-band, n: Na-band, p: p-band, b: b-band ▪ *A* (image area): f: frame that means effective area, b: optical black area
level	Product level index: l2a, l2b, l2c, l2d l2e, l2dbpc, l2drc, and l2erc

5.4 Standards Used in Generating Data Products

5.4.1 PDS Standards

All data products described in this SIS conform to PDS4 standards as described in the PDS Standards document noted in the "Applicable Documents" section of this SIS. Prior to public release, all data products will have passed a PDS peer review to ensure compliance with applicable standards.

In consultation with the PDS, the Hayabusa2 mission shall use the 1.14.0.0 version of the PDS4 information model. All Hayabusa2 products will conform to this standard, however products may have various versions of specific Discipline Dictionaries.

5.4.2 Time Standards

All Hayabusa2 ONC data products contain UTC times in their file names and header text that have been derived from the Hayabusa2 spacecraft clock time, TI. The transformation table from the spacecraft clock to UTC is provided by SIRIUS and is converted to SPICE SCLK file by the Hayabusa2 DAC team. The transformation from the spacecraft clock time to UTC time is conducted by the ONC team proprietarily using the SPICE SCLK and LSK kernels and the SPICE toolkit. However, UTC time can be converted by users to other times using standard SPICE routines with the SPICE SCLK file included in the Hayabusa2 SPICE bundle.

5.4.3 Coordinate Systems

All coordinate systems used by the Hayabusa2 mission conform to IAU standards. A complete discussion of the coordinate systems and how they are deployed in the mission can be found in Ryugu Coordinate System Description (Hirata, 2020) included in document collection of the Hayabusa2 mission bundle.

5.4.4 Data Storage Conventions

All ONC data products are stored natively as FITS files and conform to the FITS 3.0 standard (Pence et al., 2010).

5.5 Data Validation

The ONC team checks the validity of the data manually and visually when Level 2a images are created. If any pixels in the images are skipped or flipped, related data are downlinked and processed again. In order to assist this process, some statistical values, such as minimum value, maximum value, mean value, and the standard deviation of DNs within an image are automatically obtained.

The intensity histogram, FFT power spectrum and histogram equalization images are also created and checked visually by the team. The validity of the subsequent process was checked during "Landing Site Selection drill," or the data analysis training campaign using simulated asteroid images. In the campaign, the ONC team confirmed that the pipeline tool reproduces the reflectance (Level 2e) of the given asteroid model.

In addition to the software verification and validation, each data product is peer-reviewed in terms of conformity with PDS standard. No changes are expected to the data formats after the review. Should any changes be needed, nevertheless, the configuration control process will be implemented and documented (Section 3).

6 Detailed Data Product Specifications

The following sections provide detailed data product specifications for each level of ONC data product.

6.1 Data Product Structure and Organization

The Hayabusa2 data archive is organized as bundles by instrument. The ONC bundle of the archive is organized by processing level, product type and then by mission phase. Data products are stored under each mission phase directory which is just under data collection directory. Which mission phase directory is selected to store data product is determined by the value of the start_date_time attribute of the Product_Observational/Observation_Area/Time_Coordinates class being in which mission phase period. The list of collections and products in each collection is summarized in Table 20. These collections are under the Hayabusa2 ONC bundle directory, *hyb2_onc*. Each name of collection is same as directory name in the bundle.

Table 20. List of collections and products in each collection

Directory name of collection	Collection	Product in collection
browse	Browse Collection	Browse Product
calibration	Calibration Collection	Calibration Product
data_raw	Raw Data Collection	Raw / Partially Onboard Processed Image Data
data_partially_processed	Partially Processed Data Collection	Partially Processed Image Data
data_calibrated	Calibrated Data Collection	Distortion-Corrected and Physically-Converted Image Data
data_iof	I/F Data Collection	Derived I/F Image Data
data_reflectance	Reflectance Data Collection	Derived Photometrically Corrected Reflectance Image Data
data_iof_coregistered	Co-registered I/F Data Collection	Derived Co-Registered I/F Image Cube Data
data_reflectance_coregistered	Co-registered Reflectance Data Collection	Derived Co-Registered Photometrically Corrected Reflectance Image Cube Data
document	Document Collection	SIS (This file) and instrument papers
geometry	Geometry Collection	Derived Backplane Image Cube Data

All products are stored as FITS files with a detached PDS label. The detached PDS labels are PDS4 compliant XML labels that describe the contents of the file and contain all necessary metadata to interpret the product. Files can be used and viewed using standard FITS tools, and also with standard PDS4 tools. The files are:

1. **Level 2a - Raw / Partially Onboard Processed Image Data** – Images and metadata reassembled from spacecraft telemetry in units of DN at the bit depth of either of 8, 10, or 12.
2. **Level 2b – Partially Processed Image Data** – Images and metadata corrected for instrument effects (see Figure 10 for details) in unit of counts (DN converted the bit depth of 12 bit).
3. **Level 2c – Distortion-Corrected and Physically-Converted Image Data** – Images and metadata calibrated to radiance. Temperature dependent sensitivity is considered in this process. Distortion correction is also conducted for this product.
4. **Level 2d – Derived I/F Image Data** – Images converted to apparent reflectance with appropriate metadata attached.
5. **Level 2e – Derived Photometrically Corrected Reflectance Image Data** – Photometrically corrected to standard geometry images with appropriate metadata.
6. **Level 2drc – Derived Co-Registered I/F Image Cube Data** – Images converted to apparent reflectance I/F and co-registered among the bands. This product is provided as FITS-cube (band is added as the third dimension) with appropriate metadata attached.
7. **Level 2erc – Derived Co-Registered Photometrically Corrected Reflectance Image Cube Data** – Images converted to reflectance factor and co-registered among the bands. This product is provided as FITS-cube (band is added as 3rd dimension of cube) with appropriate metadata attached.
8. **Level 2dbpc – Derived Backplane Image Cube Data** – "Backplane data" (i.e., latitude, longitude, and viewing geometry parameters) for Level 2d image data. This product is also provided as FITS-cube with appropriate metadata attached.
9. **Browse Product –** These data are JPEG format data created from other data products.
10. **Calibration Data Product –** This product is calibration data used to calibrate ONC data.

6.2 Data Format Descriptions

6.2.1 Level 2a - Raw / Partially Onboard Processed Image Data

The ONC's downlinked data are images that have been reassembled from spacecraft telemetry and have instrument status and geometry information appended as metadata. The format of metadata is the same for L2a, L2b, L2c, L2d, and L2e as shown in this section. One exception is that the metadata for the sub-images is added for onboard-smear-noise corrected images and onboard-stacked images according to the number of sub images used in onboard processing. The different types of headers used for non-processed (raw) images and onboard processed images are schematically shown in Figure 18.

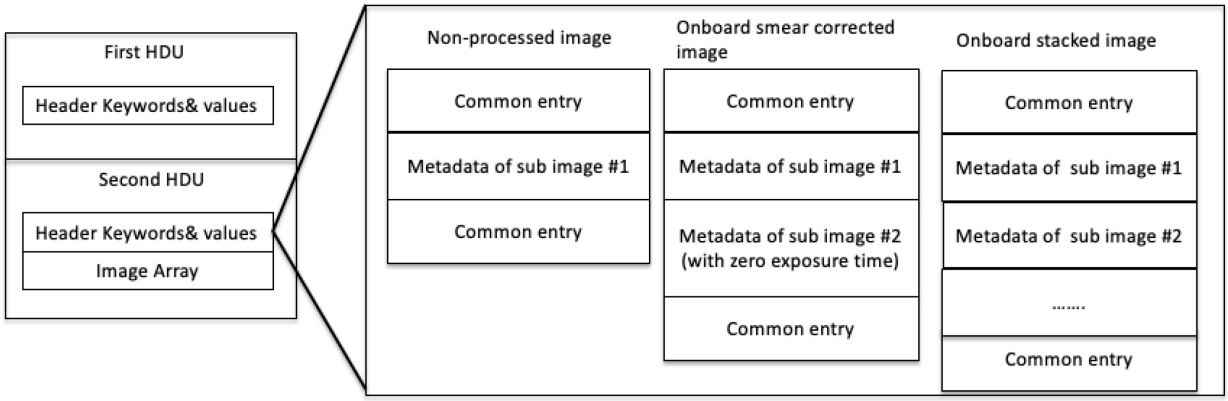

Figure 18. Difference of ONC HDU for raw data and onboard smear corrected images of ONC L2a-L2e.

A list of metadata included in the FITS files is shown in Table 21. Although the original data is 12-bit after A/D conversion, value in each pixel is stored in 16-bit signed integer, thus the amount of a frame image is about 2 MiB after decompression for L2a product.

Table 21. L2a, L2b, L2c, L2d, and L2e ONC image metadata.

PDS4 class/attribute	**FITS keyword**	**Description for FITS keyword**
Header keyword list for the primary HDU		
Not used	SIMPLE	conformity to FITS standard
Not used	BITPIX	number of bits per data pixel
Not used	NAXIS	number of data axes
Not used	EXTEND	possibility of presence of extensions
Not used	FMTTYPE	type of format in FITS file
Not used	FTYPEVER	version of FMTTYPE definition
Not used	CNTTYPE	type of data content
Not used	CNTVER	version of data content
Not used	ORIGIN	organization responsible for the data
Not used	DATE	date of generation of this HDU in UTC
Not used	TELESCOP	telescope used to acquire data
Not used	SPCECRFT	name of spacecraft
Not used	NEXTEND	number of standard extensions
File/file_name	FILENAME	original filename
hyb2:ONC_Image_Information/hyb2:observation_mode	IMGMOD	observation mode: SCIENCE for science, NAVDUMP for navigation dump
Header keyword list for the secondary HDU		
Not used	XTENSION	type of extension
Array_2D_Image/Element_Array/data_type	BITPIX	number of bits per data pixel
Array_2D_Image/axes	NAXIS	number of data axes
Array_2D_Image/Axis_Array/elements	NAXIS1	length of data axis 1
Array_2D_Image/Axis_Array/elements	NAXIS2	length of data axis 2
Not used	PCOUNT	number of parameters per group
Not used	GCOUNT	number of groups
Not used	EXTNAME	name of this HDU
Not used	EXTVER	version of the extension

PDS4 class/attribute	FITS keyword	Description for FITS keyword
Not used	ORIGIN	organization responsible for the data
File/creation_date_time	DATE	date of generation of this HDU in UTC
Time_Coordinates/start_date_time	DATE-BEG	date of the start of observation in UTC
hyb2:Observation_Information/hyb2:observation_date_time and geom:Geometry_Orbiter / geom:geometry_reference_time_utc	DATE-OBS	date of the middle of observation in UTC
Time_Coordinates/stop_date_time	DATE-END	date of the end of observation in UTC
Not used	TELESCOP	telescope used to acquire data
Not used	SPCECRFT	name of spacecraft
Not used	INSTRUME	name of instrument
Target_Identification/name	OBJECT	name of observed object
hyb2:Mission_Information/hyb2:mission_phase_name	MSNPHASE	mission phase
Not used	OPETYPE	operation type
Array_2D_Image/Element_Array/unit	BUNIT	physical units of the array values
hyb2:Image_Observation_Information/hyb2:unit_count_value	BUNITDU	quantity of this product value for 1 DU in units of [BUNIT/DU]; this value explains resolution of pixel value at this processing level
hyb2:ONC_Image_Information/hyb2:dynamic_range	DYNRNG	Dynamic range of this product [BUNIT]
hyb2:ONC_Image_Information/hyb2:linearity_guaranteed_range	DYNRNGLN	Dynamic range of this product in which linearity is guaranteed [BUNIT]
Not used	DATAMAX	maximum data value
Not used	DATAMIN	minimum data value
Not used	MEAN	mean value of the data
Not used	STDDEV	standard deviation of the data
ONC Observation Information		
hyb2:Observation_Information/hyb2:naif_instrument_name	NAIFNAME	NAIF instrument name
Not used	NAIFID	NAIF instrument ID code
hyb2:Image_Observation_Information/hyb2:exposure_duration and img:Exposure / img:exposure_duration	XPOSURE	Exposure time [s]
hyb2:Image_Observation_Information/hyb2:filter_name and used for img:Optical_Filter / img:filter_name, img:filter_id, and img:filter_number	FILTER	Filter name
hyb2:Image_Observation_Information/hyb2:band_center and img:Optical_Filter / img:center_filter_wavelength	BANDCSEL	effective band center [μ m]
hyb2:Image_Observation_Information/hyb2:bandwidth and img:Optical_Filter / img:bandwidth	BANDWSEL	effective band width [μ m]
hyb2:ONC_Instrument_Attributes/hyb2:{t,w1,t2}_ccd_temperature and img:Instrument_State / img:Device_Temperatures / img:Device_Temperature	CCDTSEL	CCD temperature for selected camera head [degC]
hyb2:ONC_Instrument_Attributes/hyb2:{t,w1,t2}_electronics_circuit_temperature and img:Instrument_State / img:Device_Temperatures / img:Device_Temperature	ELETSEL	ONC-AE temperature (same as ONC_AET) [degC]
hyb2:ONC_Image_Information/hyb2:number_of_subimage	NSUBIMG	Number of sub images
Sub-image information; i in the last character of the FITS header keyword name is for i-th sub-image.		
hyb2:ONC_Image_Information/hyb2:ONC_Sub_Image_Information/hyb2:sequence_number	-	sequence number of sub image

PDS4 class/attribute	FITS keyword	Description for FITS keyword
hyb2:ONC_Image_Information/hyb2:ONC_Sub_Image_Information/hyb2:spacecraft_clock_count	TIi	Spacecraft clock count for sub image. Note that one tick of TI is approximately equal to 1/32 seconds.
hyb2:ONC_Image_Information/hyb2:ONC_Sub_Image_Information/hyb2:analog_electronics_mode	AE_MODEi	ONC-AE mode: STDBY or SHOT
hyb2:ONC_Image_Information/hyb2:ONC_Sub_Image_Information/hyb2:digital_electronics_selection	OD_SELi	Selected digital electronics (image processor) for sub image processing; ONC-E or DE
hyb2:ONC_Image_Information/hyb2:ONC_Sub_Image_Information/hyb2:t_driving_status	T_DRVSi	ONC-T driving status: ON or OFF
hyb2:ONC_Image_Information/hyb2:ONC_Sub_Image_Information/hyb2:t_camera_selection_status	T_SELi	Camera head selection status for ONC-T
hyb2:ONC_Image_Information/hyb2:ONC_Sub_Image_Information/hyb2:t_exposure_duration	T_EXPi	Exposure time for ONC-T [s]
hyb2:ONC_Image_Information/hyb2:ONC_Sub_Image_Information/hyb2:t_filter_name	FILTERi	Filter name used for ONC-T
hyb2:ONC_Image_Information/hyb2:ONC_Sub_Image_Information/hyb2:flat_field_lamp_a_status	FFLASTi	Flatfield lamp A status
hyb2:ONC_Image_Information/hyb2:ONC_Sub_Image_Information/hyb2:flat_field_lamp_b_status	FFLBSTi	Flatfield lamp B status
hyb2:ONC_Image_Information/hyb2:ONC_Sub_Image_Information/hyb2:w1_driving_status	W1_DRVSi	ONC-W1 driving status: ON or OFF
hyb2:ONC_Image_Information/hyb2:ONC_Sub_Image_Information/hyb2:w1_camera_selection_status	W1_SELi	Camera head selection status for ONC-W1
hyb2:ONC_Image_Information/hyb2:ONC_Sub_Image_Information/hyb2:w1_exposure_duration	W1_EXPi	Exposure time for ONC-W1 [s]
hyb2:ONC_Image_Information/hyb2:ONC_Sub_Image_Information/hyb2:flash_lamp_status	FLSTATi	Flash-light status
hyb2:ONC_Image_Information/hyb2:ONC_Sub_Image_Information/hyb2:w2_driving_status	W2_DRVSi	ONC-W2 driving status: ON or OFF
hyb2:ONC_Image_Information/hyb2:ONC_Sub_Image_Information/hyb2:w2_camera_selection_status	W2_SELi	Camera head selection status for ONC-W2
hyb2:ONC_Image_Information/hyb2:ONC_Sub_Image_Information/hyb2:w2_exposure_duration	W2_EXPi	Exposure time for ONC-W2 [s]
hyb2:ONC_Image_Information/hyb2:ONC_Sub_Image_Information/hyb2:filter_wheel_driver_timeout_error_count	FWD_TECi	Filter wheel driver time out error count
hyb2:ONC_Image_Information/hyb2:ONC_Sub_Image_Information/hyb2:filter_wheel_driver_null_position_flag	FWD_NULi	Filter wheel driver null position flag: T/F
hyb2:ONC_Image_Information/hyb2:ONC_Sub_Image_Information/hyb2:filter_wheel_driver_position_sensor_status	FWD_PSTi	Filter wheel driver position sensor status ON/OFF
hyb2:ONC_Image_Information/hyb2:ONC_Sub_Image_Information/hyb2:filter_wheel_driver_reset_status	FWD_RSTi	Filter wheel driver reset status: NON or RESET
hyb2:ONC_Image_Information/hyb2:ONC_Sub_Image_Information/hyb2:filter_wheel_driver_driving_status	FWD_DRVi	Filter wheel driver driving status: STOP or RUN
hyb2:ONC_Image_Information/hyb2:ONC_Sub_Image_Information/hyb2:filter_wheel_driver_step_counter	FWD_SCEi	Filter wheel driver counter error count
hyb2:ONC_Image_Information/hyb2:ONC_Sub_Image_Information/hyb2:filter_wheel_driver_step_counter_error_count	FWD_SCi	Filter wheel driver step counter

PDS4 class/attribute	FITS keyword	Description for FITS keyword
Miscellaneous information		
hyb2:Image_Observation_Information/hyb2:number_of_binning and img:Downsampling / img:Pixel_Averaging_Dimensions / img:heigh_pixels and img:width_pixels	NPIXBIN	binning pixels: 1 (No binning), 2 (2 × 2), 4 (4 × 4), or 8 (8 × 8)
img:Subframe/img:first_sample except for optical black image	ROI_LLX	Positions of ROI image in CCD coordinates: ROI_LLX and ROI_LLY are x- and y-indexes of pixel at the lower left corner, respectively. ROI_URX and ROI_URY are x- and y-indexes of pixel at the upper right corner, respectively. All indexes are expressed in 1-based in the CCD coordinates.
img:Subframe/img:first_line	ROI_LLY	
not used	ROI_URX	
not used	ROI_URY	
hyb2:Observation_Information/hyb2:raw_file_name	L0NAME	filename of raw image at Level 0
Hayabusa2 Onboard Processing Information		
img:Onboard_Compression/img:onboard_compression_class	IMGCMPRV	Image compression class: RAW_DATA, LOSSLES, or LOSSY
img:Onboard_Compression/img:onboard_compression_type	IMGCMPAL	Image compression algorithm: RAW_DATA or STARPIXEL
img:Onboard_Compression/img:StarPixel_Lossless_Parameters/img:starpixel_initial_subsampling_interval img:Onboard_Compression/img:StarPixel_Flexible_Parameters/img:starpixel_initial_subsampling_interval	IMGCMPPR	image compression parameter: initial subsampling interval for StarPixel
img:Onboard_Compression/img:StarPixel_Flexible_Parameters/img:starpixel_degradation	IMGCMPPR	image compression parameter: quality degradation parameter for StarPixel Flexible (lossy algorithm)
hyb2:Image_Observation_Information/hyb2:image_processing_return_status	IMGPRCST	Image processing error log: "NORMAL END" or brief description of error information
HAYABUSA2 Spacecraft Clock Information		
hyb2:Observation_Information/hyb2:spacecraft_clock_start_count; This value is estimated by SCCL-BEG – int(XPOSURE*32), because the SCCL-BEG is the clock count for the end of observation of the first sub image, instead of the start of observation. The multiplication factor 32 for the XPOSURE comes from approximate one tick of TI, 1/32 seconds.	SCCL-BEG	Hayabusa2 spacecraft clock start count; Note that value of this FITS header keyword is count at the end of observation of the first sub image.
hyb2:Observation_Information/hyb2:spacecraft_clock_stop_count	SCCL-END	Hayabusa2 spacecraft clock stop count; the end of observation of the last image.
HAYABUSA2 Image Processing Information		
hyb2:Image_Observation_Information/hyb2:actual_bitdepth	BITDEPTH	bit pixel depth actually used; 12, 10, or 8
hyb2:ONC_Image_Processing_Parameters/hyb2:smear_correction_status	SMEARCR	smear correction (L2b): NON/ONBOARD/GROUND
hyb2:ONC_Image_Processing_Parameters/hyb2:bias_correction_status	BIASCR	bias correction (L2b): NON/ONBOARD/GROUND
hyb2:ONC_Image_Processing_Parameters/hyb2:dark_correction_status	DARKCR	dark correction (L2b): T/F
hyb2:ONC_Image_Processing_Parameters/hyb2:nonlinearity_correction_status	NLINERCR	non-linearity correction (L2b): T/F
hyb2:ONC_Image_Processing_Parameters/hyb2:nonlinearity_correction_file_name	LINCRCFN	non-linearity correction version (L2b)
hyb2:ONC_Image_Processing_Parameters/hyb2:flat_field_correction_status	FLATCR	flat correction: NON/CORRECTED

PDS4 class/attribute	FITS keyword	Description for FITS keyword
hyb2:ONC_Image_Processing_Parameters/hyb2:flat_field_correction_parameter_file_name	FLATCFN	flatfield database filename
hyb2:ONC_Image_Processing_Parameters/hyb2:flat_field_correction_file_name	FLATFN	flatfield filename (L2b)
hyb2:ONC_Image_Processing_Parameters/hyb2:stray_light_correction_status	STRLCR	stray light correction (L2b): T/F
hyb2:ONC_Image_Processing_Parameters/hyb2:hardware_correction_file_name and hyb2:hardware_correction_status	ELCRCFN	Filename used for electric circuit correction (L2b)
hyb2:ONC_Image_Processing_Parameters/hyb2:temperature_dependent_flat_field_correction_file_name and hyb2:temperature_dependent_flat_field_correction_status	FLATDFN	File for temperature dependent component of flatfield (L2b)
hyb2:ONC_Image_Processing_Parameters/hyb2:stray_light_mean_file_name	STRLPFN1	stray light pattern file 1; mean pattern (L2b)
hyb2:ONC_Image_Processing_Parameters/hyb2:stray_light_first_principal_component_file_name	STRLPFN2	stray light pattern file 2; first principal component (L2b)
hyb2:ONC_Image_Processing_Parameters/hyb2:stray_light_second_principal_component_file_name	STRLPFN3	stray light pattern file 3; second principal component (L2b)
hyb2:ONC_Image_Processing_Parameters/hyb2:distortion_correction_status	DISTCR	distortion correction (L2c): T/F
hyb2:ONC_Image_Processing_Parameters/hyb2:distortion_correction_file_name	DISTCFN	Filename used for distortion correction (L2c)
hyb2:ONC_Image_Processing_Parameters/hyb2:alignment_offset_correction_status	AOFFSET	alignment offset correction (L2c): T/F
hyb2:ONC_Image_Processing_Parameters/hyb2:radiance_conversion_status	RADCONV	conversion to radiance (L2c): T/F
hyb2:ONC_Image_Processing_Parameters/hyb2:radiometric_calibration_file_name and hyb2:radiometric_calibration_status	RADCCFN	radiometric calibration version (L2c)
hyb2:ONC_Image_Processing_Parameters/hyb2:ccd_sensitivity_calibration_file_name and hyb2:ccd_sensitivity_calibration_status	CCDTDCFN	CCD Temperature-dependent correction file (L2c)
hyb2:ONC_Image_Processing_Parameters/hyb2:ccd_sensitivity	SENSSEL	CCD sensitivity (L2c) [(counts/sec)/(W/m2/um/str)]
hyb2:ONC_Image_Processing_Parameters/hyb2:sensitivity_calibration_period; if value is 0, the value for this attribute is "All Periods", and if value is 1, it is "Before Touch Down 1", and if value is 2, it is "Between Touch Down 1 and Touch Down 2", and if value is 3, it is "After Touch Down 2".	SCALPRD	sensitivity calibration period: ■ 0: All periods, ■ 1: Before TD1, ■ 2: Between TD1 and TD2, and ■ 3: After TD2
hyb2:ONC_Image_Processing_Parameters/hyb2:elapsed_time_for_sensitivity_calibration	SCALDAY	Elapsed time from the start of the calibration period [day]
hyb2:ONC_Image_Processing_Parameters/hyb2:solar_distance_correction_status	SOLDISCR	solar distance correction (L2d): T/F
hyb2:ONC_Image_Processing_Parameters/hyb2:solar_distance_for_calibration	SOLDCAL	solar distance used for solar distance correction (L2d) [au]
hyb2:ONC_Image_Processing_Parameters/hyb2:effective_solar_irradiance	SOLIRRAD	effective solar irradiance at 1AU (L2d) [W/m2/um]
hyb2:ONC_Image_Processing_Parameters/hyb2:photometric_correction_status	PHOTOCR	photometric correction (L2e): T/F
hyb2:ONC_Image_Processing_Parameters/hyb2:photometric_correction_file_name	PHOTCFN	phase function file name (L2e)

PDS4 class/attribute	FITS keyword	Description for FITS keyword
Version Information of FITS Keyword Dictionary		
Not used	DICVER	version of common keyword dictionary for Hayabusa2
ONC House Keeping Data		
hyb2:ONC_Instrument_Attributes/hyb2:bus_line_voltage and and img:Imaging / img:Instrument_State / img:Device_Voltages / img:Device_Voltage	BUS_V	Bus line voltage [V]
hyb2:ONC_Instrument_Attributes/hyb2:onc_electric_current and img:Imaging / img:Instrument_State / img:Device_Currents / img:Device_Current	ONC_I	ONC current value [A]
hyb2:ONC_Instrument_Attributes/hyb2:fla_c_electric_current and img:Imaging / img:Instrument_State / img:Device_Currents / img:Device_Current	FLAC_I	FLA-C current value [A]
hyb2:ONC_Instrument_Attributes/hyb2:onc_analog_electronics_temperature and img:Imaging / img:Instrument_State / img:Device_Temperatures / img:Device_Temperature	ONC_AET	ONC-AE temperature [degC]
hyb2:ONC_Instrument_Attributes/hyb2:t_optics_temperature and img:Imaging / img:Instrument_State / img:Device_Temperatures / img:Device_Temperature	T_OPTT	ONC-T optics temperature [degC]
hyb2:ONC_Instrument_Attributes/hyb2:t_ccd_temperature and img:Imaging / img:Instrument_State / img:Device_Temperatures / img:Device_Temperature	T_CCDT	ONC-T CCD temperature [degC]
hyb2:ONC_Instrument_Attributes/hyb2:t_electric_circuit_temperature and img:Imaging / img:Instrument_State / img:Device_Temperatures / img:Device_Temperature	T_ELET	ONC-T electric circuit temperature [degC]
hyb2:ONC_Instrument_Attributes/hyb2:w1_optics_temperature and img:Imaging / img:Instrument_State / img:Device_Temperatures / img:Device_Temperature	W1_OPTT	ONC-W1 optics temperature [degC]
hyb2:ONC_Instrument_Attributes/hyb2:w1_ccd_temperature and img:Imaging / img:Instrument_State / img:Device_Temperatures / img:Device_Temperature	W1_CCDT	ONC-W1 CCD temperature [degC]
hyb2:ONC_Instrument_Attributes/hyb2:w1_electric_circuit_temperature and img:Imaging / img:Instrument_State / img:Device_Temperatures / img:Device_Temperature	W1_ELET	ONC-W1 electric circuit temperature [degC]
hyb2:ONC_Instrument_Attributes/hyb2:w2_optics_temperature and img:Imaging / img:Instrument_State / img:Device_Temperatures / img:Device_Temperature	W2_OPTT	ONC-W2 optics temperature [degC]
hyb2:ONC_Instrument_Attributes/hyb2:w2_ccd_temperature and img:Imaging / img:Instrument_State / img:Device_Temperatures / img:Device_Temperature	W2_CCDT	ONC-W2 CCD temperature [degC]
hyb2:ONC_Instrument_Attributes/hyb2:w2_electric_circuit_temperature and img:Imaging / img:Instrument_State / img:Device_Temperatures / img:Device_Temperature	W2_ELET	ONC-W2 electric circuit temperature [degC]
hyb2:ONC_Instrument_Attributes/hyb2:fla_c_temperature and img:Imaging / img:Instrument_State / img:Device_Temperatures / img:Device_Temperature	FLAC_T	FLA-C temperature [degC]
HYB2 Geometry Information at observation		
hyb2:Observation_Geometry/hyb2:ryugu_distance_from_spacecraft and geom:Geometry_Orbiter / geom:Distances / geom:Distances_Specific /	S_DISTHR	distance between Hayabusa2 and Ryugu [km]

PDS4 class/attribute	FITS keyword	Description for FITS keyword
geom:spacecraft_central_body_distance and geom:spacecraft_target_center_distance		
hyb2:Observation_Geometry/hyb2:earth_distance_from_spacecraft and geom:Geometry_Orbiter / geom:Distances / geom:Distances_Specific / geom:spacecraft_geocentric_distance	S_DISTHE	distance between Hayabusa2 and Earth [km]
hyb2:Observation_Geometry/hyb2:sun_distance_from_spacecraft and geom:Geometry_Orbiter / geom:Distances / geom:Distances_Specific / geom:spacecraft_heliocentric_distance	S_DISTHS	distance between Hayabusa2 and the Sun [km]
hyb2:Observation_Geometry/hyb2:sun_distance_from_ryugu and geom:Geometry_Orbiter / geom:Distances / geom:Distances_Specific / geom:target_heliocentric_distance	S_DISTRS	distance between Ryugu and the Sun [km]
Not Used	S_TGRADI	Ryugu radius at the equator [km]
Not Used	S_APPDIA	apparent diameter of Ryugu seen from the spacecraft [deg]
geom:Geometry_Orbiter / geom:Pixel_Dimension / geom:horizontal_pixel_field_of_view and geom:vertical_pixel_field_of_view	S_IFOV	instantaneous field of view [rad]
Not used	S_SOLLAT	sub solar latitude [deg] of Ryugu
Not used	S_SOLLON	sub solar longitude (0–360) [deg] of Ryugu
Not used	S_SSCLAT	sub S/C latitude [deg] of Ryugu
Not used	S_SSCLON	sub S/C longitude (0–360) [deg] of Ryugu
Not used	S_SSCLT	sub S/C local time [h] of Ryugu
hyb2:Observation_Geometry / hyb2:spacecraft_x_position, hyb2:spacecraft_y_position, and hyb2:spacecraft_z_position, and geom:Geometry_Orbiter / geom:Vectors / geom:Vectors_Cartesian_Specific / geom:Vector_Cartesian_Position_Sun_To_Spacecraft / geom:x_position, geom:y_position, and geom:z_position	S_SCPJ2X	x- (S_SCPJ2X), y- (S_SCPJ2Y), and z- (S_SCPJ2Z) components of Spacecraft position from the Sun in J2000 [km]
	S_SCPJ2Y	
	S_SCPJ2Z	
RA/DEC Information at observation		
geom:right_ascension_angle and geom_declination_angle attributes in geom:Geometry / geom:Image_Display_Geometry / geom:Object_Orientation_RA_Dec class. If value of the geom:reference_pixel_location attribute in the geom:Object_Orientation_RA_Dec class is Center, Lower Left Corner, Lower Right Corner, Upper Left Corner, or Upper Right Corner, the value of geom:right_ascension_angle and geom_declination_angle is (S_RA, S_DEC), (S_RA1, S_DEC1), (S_RA2, S_DEC2), (S_RA3, S_DEC3), or (S_RA4, S_DEC4), respectively.	S_RA	Right Ascension and Declination in degrees in J2000 for the image at the center (S_RA, S_DEC), the lower left corner (S_RA1, S_DEC1), the lower right corner (S_RA2, S_DEC2), the upper left corner (S_RA3, S_DEC3), and the upper right corner (S_RA4, S_DEC4).
	S_DEC	
	S_RA1	
	S_DEC1	
	S_RA2	
	S_DEC2	
	S_RA3	
	S_DEC3	
	S_RA4	
	S_DEC4	
S/C Attitude information at observation and related information		
hyb2:Observation_Geometry/hyb2:sun_direction_spacecraft_x_axis_angle, hyb2:sun_direction_spacecraft_y_axis_angle, and hyb2:sun_direction_spacecraft_z_axis_angle	S_SCXSAN	angle of S/C x-axis (S_SCXSAN), y-axis (S_SCYSAN), and z-axis (S_SCZSAN) and the Sun direction [deg]
	S_SCYSAN	
	S_SCZSAN	

PDS4 class/attribute	FITS keyword	Description for FITS keyword
hyb2:ONC_Image_Information/hyb2:first_rotation_angle_for_stray_light; if value is -1000, it represents missing value.	S_SCPHAN	angle of S/C twisting relative to the nominal observation attitude, φ [deg]
hyb2:ONC_Image_Information/hyb2:second_rotation_angle_for_stray_light; if value is -1000, it represents missing value.	S_SCGMAN	angle of S/C twisting relative to the nominal observation attitude, γ [deg]
hyb2:ONC_Image_Information/hyb2:stray_light_status	S_SLFLG	stray light flag for ONC-T
SPICE KERNELS		
Not used. Will be used in future if value is correctly filled.	S_PCK	SPICE PCK filename
	S_LSK	SPICE LSK filename
	S_IK	SPICE IK filename
	S_SPK	SPICE SPK filename
	S_FK	SPICE FK filename
	S_SCL	SPICE SCLK filename
	S_CK	SPICE CK filename
Backplane related keyword		
geom:Surface_Geometry / geom:Surface_Geometry_Specific / geom:Pixel_Intercept / geom:pixel_latitude and geom:pixel_longitude	M_FCLAT	latitude (M_FCLAT) and longitude (0–360) (M_FCLON) of target body at the center of image in degrees
	M_FCLON	
geom:Gometry_Orbiter / geom:Pixel_Dimensions / geom:Pixel_Size_Projected / geom:distance	M_FCDIST	distance [m] of target body at the center of image.
geom:Geometry_Orbiter / geom:Pixel_Dimensions / geom:Pixel_Size_Projected / geom:horizontal_pixel_footprint and geom:vertical_pixel_footprint	M_FCRES	spatial resolution of 1 pixel on the surface of target body at the center of image [m/pixel]
geom:Surface_Geometry / geom:Surface_Geometry_Specific / geom:Pixel_Intercept / geom:pixel_latitude and geom:pixel_longitude	M_4CNLAT	latitude (M_4CNLAT) and longitude (0–360) (M_4CNLON) of target body for reticle points of image in degrees
	M_4CNLON	
hyb2:Observation_Geometry/hyb2:backplane_data_version	M_VER	version of backplane data
hyb2:Observation_Geometry/hyb2:backplane_spice_kernel_file_name	M_MKERN1	SPICE MK file names used to create backplane data
	M_MKERN2	
	M_MKERN3	
hyb2:Observation_Geometry/hyb2:backplane_shape_model_spice_kernel_file_name	M_DSK	SPICE DSK used to create backplane data
hyb2:Observation_Geometry/hyb2:backplane_file_name	M_BPFIL	backplane file name for this image

6.2.2 Level 2b – Partially Processed Image Data

The format of Level 2b (Partially Processed Image Data) is the same as that of Level 2a, except that the image data is converted into 32-bit float through the ground calibration (see Section 5.3.2.2). The data amount for a frame is about 4 MiB.

6.2.3 Level 2c – Distortion-Corrected and Physically Converted Image Data

The format of Level 2c (Distortion Corrected and Physically Converted Image Data) is the same with Level 2b except that some of the values of related header attributes are filled or changed due to data processing. The pixels that cannot be sampled during distortion correction is filled with zero.

6.2.4 Level 2d – Derived I/F Image Data

The format of Level 2d (Derived I/F Image Data) is the same with Level 2c except for that some of the values of related header attributes such as filenames used for calibration or calibration status are filled or changed due to data processing.

6.2.5 Level 2e - Derived Photometrically Corrected Reflectance Image Data

The format of Level 2e (Derived Photometrically Corrected Reflectance Image Data) is the same with Level 2c except that some of the values of related attributes are filled or changed due to data processing. Parameters used for photometric correction (e.g., parameters of Hapke's model), shape model, and SPICE kernels used to create backplane data, have been added.

6.2.6 Level 2dbpc - Derived Backplane Cube Data

The format of Level 2dbpc (Derived Backplane Cube Data applicable to L2c, L2d, and L2e) is composed of primary HDU and secondary HDU as shown in Figure 19. The secondary HDU includes longitude, latitude, range, viewing geometry parameters, and Polygon IDs as a 3-dimensional matrix composed of 7 images. The header the primary HDU of Level 2dbpc is almost the same as those of L2c or L2d. The header of the secondary HDU is simplified to include standard FITS header keywords, contents and units of each layer, and the backplane-related data such as SPICE SPK file and shape files used to calculate data.

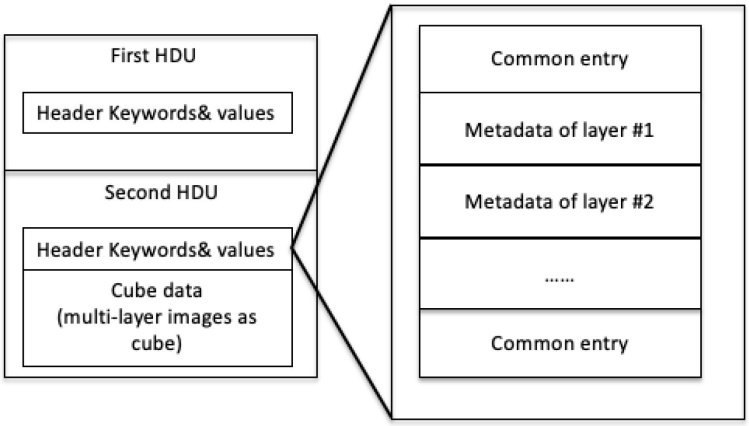

Figure 19. HDU for cube data of ONC L2dbpc, L2drc, and L2erc.

A list of metadata included in the FITS-cube is shown in Table 22. Each pixel of the data is 32-bit floating-point number, thus the amount of the data of one L2dbpc file is approximately 28 MiB.

Table 22. L2dbpc ONC image metadata.

PDS4 attribute name	FITS keyword	Description for FITS keyword
Header keyword list for HDU #1:		
Not used	SIMPLE	conformity to FITS standard
Not used	BITPIX	number of bits per data pixel
Not used	NAXIS	number of data axes
Not used	EXTEND	possibility of presence of extensions
Not used	FMTTYPE	type of format in FITS file
Not used	FTYPEVER	version of FMTTYPE definition
Not used	CNTTYPE	type of data content
Not used	CNTVER	version of data content

PDS4 attribute name	FITS keyword	Description for FITS keyword
Not used	ORIGIN	organization responsible for the data
Not used	DATE	date of generation of this HDU in UTC
Not used	TELESCOP	telescope used to acquire data
Not used	SPCECRFT	name of spacecraft
Not used	NEXTEND	number of standard extensions
File/file_name	FILENAME	original filename
HYB2 IMG DB Information		
Not used	IMGMOD	image type: SCIENCE/NAVDUMP
Header keyword list for HDU #2:		
Not used	XTENSION	type of extension
Array_2D/Element_Array/data_type	BITPIX	number of bits per data pixel
Not used	NAXIS	number of data axes
Array_2D/Axis_Array/elements	NAXIS1	length of data axis 1
Array_2D/Axis_Array/elements	NAXIS2	length of data axis 2
Used for number of sequences of Array_2D class	NAXIS3	length of data axis 3
Not used	PCOUNT	number of parameters per group
Not used	GCOUNT	number of groups
Not used	EXTNAME	name of this HDU
Not used	EXTVER	version of the extension
Not used	ORIGIN	organization responsible for the data
File/creation_date_time	DATE	date of generation of this HDU in UTC
Time_Coordinates/start_date_time	DATE-BEG	date of the start of observation in UTC
hyb2:Observation_Information/hyb2:observation_date_time and geom:Geometry_Orbiter / geom:geometry_reference_time_utc	DATE-OBS	date of the middle of observation in UTC
Time_Coordinates/stop_date_time	DATE-END	date of the end of observation in UTC
Not used	TELESCOP	telescope used to acquire data
Not used	SPCECRFT	name of spacecraft
Not used	INSTRUME	name of instrument
Target_Identification/name	OBJECT	name of observed object
hyb2:Mission_Information/hyb2:mission_phase_name	MSNPHASE	mission phase
Not used	OPETYPE	operation type
ONC observation information		
Not used	NAIFNAME	SPICE instrument name
Not used	NAIFID	SPICE instrument ID
Not used	XPOSURE	exposure time [sec]
Not used	FILTER	selected filter of ONC-T
Not used	NPIXBIN	binning pixels: 1 (No binning), 2 (2 × 2), 4 (4 × 4), or 8 (8 × 8)
Not used	ROI_LLX	x of lower left of ROI in detector coordinates (1-based)
Not used	ROI_LLY	y of lower left of ROI in detector coordinates (1-based)

PDS4 attribute name	FITS keyword	Description for FITS keyword
Not used	ROI_URX	x of upper right of ROI in detector coordinates (1-based)
Not used	ROI_URY	y of upper right of ROI in detector coordinates (1-based)
HAYABUSA2 Image Processing Information		
Not used	DISTCFN	distortion and alignment offset correction database file version (L2c)
Not used	DICVER	version of common keyword dictionary for Hayabusa2
Not used	DISTCR	distortion correction (L2c): T/F
Not used	AOFFSET	alignment offset correction (L2c): T/F
Not used	M_VER	version of backplane data
geom:Surface_Geometry / geom:Surface_Geometry_Specific / geom:Pixel_Intercept / geom:pixel_latitude and geom:pixel_longitude	M_FCLAT	latitude (M_FCLAT) and longitude (0–360) (M_FCLON) of target body at the center of image in degrees
	M_FCLON	
geom:Gometry_Orbiter / geom:Pixel_Dimensions / geom:Pixel_Size_Projected / geom:distance	M_FCDIST	distance [m] of target body at the center of image.
geom:Geometry_Orbiter / geom:Pixel_Dimensions / geom:Pixel_Size_Projected / geom:horizontal_pixel_footprint and geom:vertical_pixel_footprint	M_FCRES	spatial resolution of 1 pixel on the surface of target body at the center of image [m/pixel]
geom:Surface_Geometry / geom:Surface_Geometry_Specific / geom:Pixel_Intercept / geom:pixel_latitude and geom:pixel_longitude	M_4CNLAT	latitude (M_4CNLAT) and longitude (0–360) (M_4CNLON) of target body for reticle points of image in degrees
	M_4CNLON	
Not used	M_MKERN1	SPICE MK file names used to create backplane data
	M_MKERN2	
	M_MKERN3	
Not used	M_DSK	SPICE DSK used to create backplane data
Not used	M_BPFIL	backplane file name
Definition of Layers		
Array_2D/name	BNAME1	Content name for layer 1
Array_2D/Element_Array/unit	BUNIT1	Unit for layer 1
Array_2D/name	BNAME2	Content name for layer 2
Array_2D/Element_Array/unit	BUNIT2	Unit for layer 2
Array_2D/name	BNAME3	Content name for layer 3
Array_2D/Element_Array/unit	BUNIT3	Unit for layer 3
Array_2D/name	BNAME4	Content name for layer 4
Array_2D/Element_Array/unit	BUNIT4	Unit for layer 4
Array_2D/name	BNAME5	Content name for layer 5
Array_2D/Element_Array/unit	BUNIT5	Unit for layer 5
Array_2D/name	BNAME6	Content name for layer 6
Array_2D/Element_Array/unit	BUNIT6	Unit for layer 6
Array_2D/name	BNAME7	Content name for layer 7
Array_2D/Element_Array/unit	BUNIT7	Unit for layer 7

6.2.7 Level 2drc – Co-registered I/F Image Cube Data

Level 2drc (Co-registered I/F Image Cube Data) is a bundle of spatially co-registered multi-band images and consecutively shot single-band images. The structure of L2drc is similar to that of L2dbpc shown in Figure 19, although the contents of cube data and metadata are different from L2dbpc. The list of metadata included in the FITS file is shown in Table 23. The header list of primary HDU is the same as the L2a-e; the header of secondary HDU is simplified to include the information describing which band is included in which layer, and which band is used as the reference while co-registering. Only the information of the reference image used for co-registration is extracted to represent the L2drc image. This information includes longitude and latitude of target body at the center of the FOV. Each pixel of the data is 32-bit floating-point number, thus the amount of the image for a frame data is approximately 28 MiB.

Table 23. L2drc and L2erc ONC image metadata

PDS4 attribute name	FITS keyword	Description for FITS keyword
Header listing for HDU #1:		
Not used	SIMPLE	conformity to FITS standard
Not used	BITPIX	number of bits per data pixel
Not used	NAXIS	number of data axes
Not used	EXTEND	possibility of presence of extensions
Not used	FMTTYPE	type of format in FITS file
Not used	FTYPEVER	version of FMTTYPE definition
Not used	CNTTYPE	type of data content
Not used	CNTVER	version of data content
Not used	ORIGIN	organization responsible for the data
Not used	DATE	date of generation of this HDU in UTC
Not used	TELESCOP	telescope used to acquire data
Not used	SPCECRFT	name of spacecraft
Not used	NEXTEND	number of standard extensions
File/file_name	FILENAME	original filename
Header listing for HDU #2:		
Not used	XTENSION	type of extension
Array_3D_Image/Element_Array/data_type	BITPIX	number of bits per data pixel
Not used	NAXIS	number of data axes
Array_3D_Image/Axis_Array/elements	NAXIS1	length of data axis 1
Array_3D_Image/Axis_Array/elements	NAXIS2	length of data axis 2
Array_3D_Image/Axis_Array/elements	NAXIS3	length of data axis 3
Not used	PCOUNT	number of parameters per group
Not used	GCOUNT	number of groups
Not used	EXTNAME	name of this HDU
Not used	EXTVER	version of the extension
Not used	ORIGIN	organization responsible for the data
File/creation_date_time	DATE	date of generation of this HDU in UTC

PDS4 attribute name	FITS keyword	Description for FITS keyword
Not used. For Time_Coordinates/start_date_time, earliest value among DATE-BE[1-7] is used.	DATE-BEG	date of the start of observation in UTC for reference band
geom:Geometry_Orbiter / geom:geometry_reference_time_utc	DATE-OBS	date of the middle of observation in UTC for reference band
Not used. For Time_Coordinates/stop_date_time, latest value among DATE-EN[1-7] is used.	DATE-END	date of the end of observation in UTC for reference band
Not used	TELESCOP	telescope used to acquire data
Not used	SPCECRFT	name of spacecraft
Not used	INSTRUME	name of instrument
Target_Identification/name	OBJECT	name of observed object
hyb2:Mission_Information/hyb2:mission_phase_name	MSNPHASE	mission phase
Not used	OPETYPE	operation type
ONC observation information		
Not used	NAIFNAME	NAIF instrument name
Not used	NAIFID	NAIF instrument ID code
Miscellaneous Information of Reference Image		
img:Subframe/img:first_sample	ROI_LLX	x of lower left point of region of interest in CCD coordinates(1-based)
Img:Subframe/img:first_line	ROI_LLY	y of lower left point of region of interest in CCD coordinates(1-based)
Not used	ROI_URX	x of upper right point of region of interest in CCD coordinates(1-based)
Not used	ROI_URY	y of upper right point of region of interest in CCD coordinates(1-based)
Not used	DISTCFN	distortion and alignment offset correction database file version(L2c)
hyb2:ONC_Multiband_Observation_Information/hyb2:stray_light_status	S_SLFLG	stray light flag for ONC-T: T/F
hyb2:ONC_Multiband_Observation_Information /hyb2:distortion_correction_status	DISTCR	distortion correction (L2c): T/F
hyb2:ONC_Multiband_Observation_Information /hyb2:alignment_offset_correction_status	AOFFSET	alignment offset correction (L2c): T/F
Backplane Related keyword for Reference Image		
hyb2:ONC_Multiband_Observation_Information/hyb2:backplane_data_version	M_VER	version of backplane data
geom:Surface_Geometry/geom:Surface_Geometry_Specific/geom:Pixel_Intercept/geom:pixel_latitude and geom:pixel_longitude	M_FCLAT	latitude (M_FCLAT) and longitude (0–360) (M_FCLON) of target body at the center of image in degrees
	M_FCLON	
hyb2:ONC_Multiband_Observation_Information/hyb2:distance_to_ryugu_at_center	M_FCDIST	distance [m] of target body at the center of image
hyb2:ONC_Multiband_Observation_Information/hyb2:spatial_resolution_of_ryugu_at_center	M_FCRES	spatial resolution of 1 pixel on the surface of target body at the center of image [m/pixel]
geom:Surface_Geometry/geom:Surface_Geometry_Specific/geom:Pixel_Intercept/geom:pixel_latitude and geom:pixel_longitude	M_4CNLAT	latitude (M_4CNLAT) and longitude (0–360) (M_4CNLON) of target body for reticle points of image in degrees
	M_4CNLON	
	M_MKERN1	

PDS4 attribute name	FITS keyword	Description for FITS keyword
hyb2:ONC_Multiband_Observation_Information /hyb2:backplane_spice_kernel_file_name	M_MKERN2	SPICE MK file names used to create backplane data
	M_MKERN3	
hyb2:ONC_Multiband_Observation_Information /hyb2:backplane_shape_model_spice_kernel_file_name	M_DSK	SPICE DSK used to create backplane data
hyb2:ONC_Multiband_Observation_Information /hyb2:backplane_file_name	M_BPFIL	backplane file (for a reference band of this cube)
used to calculate hyb2:reference_frame_filter_axis_number and hyb2:reference_frame_filter_name attributes in hyb2:ONC_Multiband_Observation_Information class, and img:array_band_number	REFFRM	Reference frame for co-registration
Keywords for each band; 01 in the keywords below is suffix for band 1. For bands 2, 3, …, the suffixes are 02, 03, ...		
hyb2:Multiband_Observation_Information/hyb2:ONC_Band_Information/hyb2:band_file_name	FNAME01	L2d filename (band 1)
Array_3D_Image/Element_Array/unit	BUNIT01	physical units of the array values
hyb2:Multiband_Observation_Information/hyb2:ONC_Band_Information/hyb2:exposure_duration	XPOSUR01	exposure time (band 1) [sec]
hyb2:Multiband_Observation_Information/hyb2:ONC_Band_Information/hyb2:filter_name	FILTER01	filter of ONC-T (band 1)
hyb2:Multiband_Observation_Information/hyb2:ONC_Band_Information/hyb2:observation_start_date_time	DATE-B01	date of the start of observation in UTC
hyb2:Multiband_Observation_Information/hyb2:ONC_Band_Information/hyb2:observation_date_time	DATE-O01	date of the middle of observation in UTC
hyb2:Multiband_Observation_Information/hyb2:ONC_Band_Information/hyb2:observation_stop_date_time	DATE-E01	date of the end of observation in UTC
hyb2:Multiband_Observation_Information/hyb2:ONC_Band_Information/hyb2:flat_field_lamp_a_status	FFLAST01	Flatfield lamp A status (band 1)
hyb2:Multiband_Observation_Information/hyb2:ONC_Band_Information/hyb2:flat_field_lamp_b_status	FFLBST01	Flatfield lamp B status (band 1)
hyb2:Multiband_Observation_Information/hyb2:ONC_Band_Information/hyb2:data_maximum	DATAMA01	maximum data value (band 1)
hyb2:Multiband_Observation_Information/hyb2:ONC_Band_Information/hyb2:data_minimum	DATAMI01	minimum data value (band 1)
hyb2:Multiband_Observation_Information/hyb2:ONC_Band_Information/hyb2:data_mean	MEAN01	mean value of the data (band 1)
hyb2:Multiband_Observation_Information/hyb2:ONC_Band_Information/hyb2:data_standard_deviation	STDDEV01	standard deviation of the data (band 1)
Keywords for the other bands/images follow in the same way.		

6.2.8 Level 2erc - Co-registered Reflectance Image Cube Data

The format of Level 2erc (Co-Registered Photometrically Corrected Reflectance Cube Data) is the same with L2drc except for the contents of the data is created from L2e instead of L2d.

6.2.9 ONC Special Pixel Values

Not assigned yet. Note that the pixels which have zero value in the L2c data are not sampled during distortion correction.

6.2.10 ONC Calibration File Formats

6.2.10.1 ONC Calibration Image Format

This section describes image format which are required for ONC flatfield correction and ONC-T's radiator stray light correction.

Flatfield data is firstly provided as normalized images of constant light sources at the room CCD temperature (e.g., an integration sphere or flat panels obtained during the ground test) for all of ONC-T, ONC-W1, and ONC-W2. Then inflight flatfields are created only for ONC-T. Inflight flatfields are created by stacking images obtained during the asteroid proximity phase (hovering at the altitude of 3 km after MASCOT release) at the CCD temperature of -30 degC. Furthermore, their temperature dependence was obtained by comparing ground flatfields and inflight flatfields at the different CCD temperature. These flatfields and CCD temperature dependence of flatfields are provided in 32-bit float FITS image, which images are used to create flatfield at a given CCD temperature and to produce L2b image products.

ONC-T's radiator stray light pattern images are obtained by a principal component analysis for a collection of various images obtained at the different attitude relative to Sun. The patterns are provided as a mean of the stray light pattern and the first and the second principal component. Currently only the mean and the first component are used to obtain the stray light pattern at a given spacecraft attitude.

These ONC calibration images are identified with file names in the format of:

hyb2_onc_c_*type_sub_CBA_x*_v*VV_yyyymmdd*.{fit, xml}

The common definition of symbols is described in Table 24. Thus, there are four types of images for each correction as listed below:

- Flatfields
  - hyb2_onc_c_flat_bse_*CBA_x*_v*VV_yyyymmdd*.{fit, xml}: base at CCD temperature of -30 degC
  - hyb2_onc_c_flat_pc1_*CBA_x*_v*VV_yyyymmdd*.{fit, xml}: CCD temperature dependent component
- Radiator stray light pattern
  - hyb2_onc_c_strl_mea_*CBA_x*_v*VV_yyyymmdd*.{fit, xml}: mean
  - hyb2_onc_c_strl_pc1_*CBA_x*_v*VV_yyyymmdd*.{fit, xml}: spacecraft attitude dependent component

Table 24. Definition of ONC calibration image filename.

No.	Symbol	Contents
1	*type*	Type of the calibration image. flat: flatfields, strl: straylight pattern of ONC-T
2	*sub*	Subtype of the calibration image. bse: base file for flatfield mea: mean pattern file for stray light pc1: a first principal component related to temperature or spacecraft attitude.
3	*CBA*	Camera type (+ band included for ONC-T) *CB* + Image area *A* *CB*: w1: ONC-W1, w2: ONC-W2, tu: ul-band of ONC-T, tv: v-band of ONC-T, tw: w-band of ONC-T, tx: x-band of ONC-T, tn: Na-band of ONC-T, tp: p-band of ONC-T, tb: b-band of ONC-T, a: all bands of ONC-T [1] *A*: f: frame, b: optical black
4	*x*	Image area, f: full, t: trimmed during co-registration among the bands
5	*VV*	Version number
6	*yyyymmdd*	Date of creation

[1] Index "a" is used only for the radiator stray light pattern of ONC-T because this pattern is known to be the same for all bands of ONC-T (Tatsumi et al., 2019a).

Table 25 shows entries of headers of flatfield correction files.

Table 25. ONC calibration image data FITS header format

PDS4 attribute name	Keyword	Description for FITS keyword
Header listing for HDU #1:		
Not used	SIMPLE	conformity to FITS standard
Not used	BITPIX	number of bits per data pixel
Not used	NAXIS	number of data axes
Not used	EXTEND	possibility of presence of extensions
Not used	FMTTYPE	type of format in FITS file
Not used	FTYPEVER	version of FMTTYPE definition
Not used	CNTTYPE	type of data content
Not used	CNTVER	version of data content
Not used	ORIGIN	organization responsible for the data
Not used	DATE	date of generation of this HDU in UTC
Not used	TELESCOP	telescope used to acquire data
Not used	SPCECRFT	name of spacecraft
Not used	NEXTEND	number of standard extensions
File/file_name	FILENAME	original filename
Header listing for HDU #2:		
Not used	XTENSION	Image extension

PDS4 attribute name	Keyword	Description for FITS keyword
Array_2D_Image/Element_Array/data_type	BITPIX	array data type
Array_2D_Image/axes	NAXIS	number of array dimensions
Array_2D_Image/Axis_Array/elements	NAXIS1	length of data axis 1
Array_2D_Image/Axis_Array/elements	NAXIS2	length of data axis 2
Not used	PCOUNT	number of parameters
Not used	GCOUNT	number of groups
Not used	EXTNAME	name of this HDU
Not used	EXTVER	version of the extension
Not used	ORIGIN	organization responsible for the data
File/creation_date_time	DATE	date of generation of this HDU in UTC
Not used	TELESCOP	telescope used to acquire data
Not used	SPCECRFT	name of spacecraft
Not used	INSTRUME	name of instrument
Array_2D_Image/Element_Array/unit	BUNIT	physical units of the array values
hyb2:Observation_Information/hyb2:naif_instrument_name	NAIFNAME	NAIF instrument name
Not used	NAIFID	NAIF instrument ID code
hyb2:Image_Observation_Information.filter_name	FILTER	selected filter of ONC-T
hyb2:ONC_Calibration_Data_Information/hyb2:ccd_temperature	CCDSEL	selected CCD temperature [degC]
hyb2:ONC_Calibration_Data_Information/hyb2:normalization	NORM	normalization T/F
hyb2:ONC_Calibration_Data_Information/hyb2:image_area_trimming	TRIM	trimming because of co-registration T/F
hyb2:ONC_Image_Processing_Parameters/hyb2:sensitivity_calibration_period; if value is 0, the value for this attribute is “All Periods”, and if value is 1, it is “Before Touch Down 1”, and if value is 2, it is “Between Touch Down 1 and Touch Down 2”, and if value is 3, it is “After Touch Down 2”.	SCALPRD	sensitivity calibration period: ■ 0: All periods, ■ 1: Before TD1, ■ 2: Between TD1 and TD2, and ■ 3: After TD2
used for Source_Product_Internal/lidvid_reference	OFNAME1	Source file name 1
used for Source_Product_Internal/lidvid_reference	OFNAME2	Source file name 2
used for Source_Product_Internal/lidvid_reference	OFNAME3	Source file name 3
used for Source_Product_Internal/lidvid_reference	OFNAME4	Source file name 4
used for Source_Product_Internal/lidvid_reference	OFNAME5	Source file name 5
used for Source_Product_Internal/lidvid_reference	OFNAME6	Source file name 6

6.2.10.2 ONC Hot pixel Identification Format

There are bad (hot) pixels in ONC’s CCD, which have the higher signals compared with the normal pixels, particularly at the higher temperature. ONC’s hot pixel information is provided as the dark signals (i.e., a map of the pixels damaged by cosmic ray and yielding unreliable values particularly at high CCD temperature) in a 32-bit float FITS image format. These images are constructed from multiple inflight observations of stars at the CCD temperature ranging from -30 degC to 30 degC. We tentatively define “hot pixels” as those yielding values more than 50 count/s for dark observation and prepared the mask images in which the values of the hot pixels are equal to 1, whereas the values of normal pixels are zero, together with raw dark images at various CCD

temperatures. Although the effect of the hot pixels is not considered in the current product, the users who are willing to conduct precise analysis can use this dataset.

These ONC hot pixel related images are identified with file names in the format of:

- hyb2_onc_c_dark_raw_*CBA_TTT_yyyymmdd*.{fit, xml}: raw dark signal image for hot pixel identification
- hyb2_onc_c_dark_bpx_*CBA_TTT_yyyymmdd*.{fit, xml}: hot pixel mask image

The common definition of symbols for both types of images is described in Table 26. The entries of headers of the hot pixel images are same with the entries of other calibration images as shown in Table 25.

Table 26. Definition of ONC hot pixel image file suffix.

No.	Symbol	Contents
1	*type*	raw: dark signal image in count/s. bpx: mask image in which the values of hot pixels are 1 otherwise 0, where hot pixels are defined as the pixels having the dark signal of 50 count/s.
2	*CBA*	Camera type (+ band for T) *CB* + Image area *A* (see Table 24)
3	*TTT*	CCD temperature [degC]
4	*yyyymmdd*	Date of creation

6.2.10.3 ONC Other Calibration Data Format

Other ONC calibration data is provided as CSV database file (.db). The typical format of such database file is shown in Figure 20. Calibration data are provided as an ASCII text file with header and data. Information of the attributes of the data is described in the comment fields in the leading part of the file and is also provided in XML label.

```
#  Version yyyymmdd comment
# Date:
# Creator:
# ….
#
#@ attribute
#Camera  (or Band)
#Description of the first attribute  (Camera or bands) :  type
#Description of the second attribute : type
#Description of the third attribute …: type
#@data
T,    value1, value2, ...
W1,  value1, value2, ...
W2,  value1, value2, ...
```

Figure 20. Typical Format of calibration database File.

A Table 27 shows a list of database files prepared for calibration. Examples of current database files are shown as Figure 21, Figure 22, Figure 23, Figure 24, Figure 25, Figure 26, Figure 27, Figure 28, Figure 29, and Figure 30 in Appendix 8.3.

Table 27. List of ONC calibration database files

File Name	Description
hyb2_onc_c_all_*yyyymmdd*.{db,xml}	List of all calibration files used to calibrate data
hyb2_onc_c_elec_*yyyymmdd*.{db,xml}	List of parameters related to electric circuits correction for each of ONC-T, ONC-W1, and ONC-W2
hyb2_onc_c_linc_*yyyymmdd*.{db,xml}	List of parameters related to linearity correction for each of ONC-T, ONC-W1, and ONC-W2.
hyb2_onc_c_flat_*yyyymmdd*.{db,xml}	List of flatfield file names for all bands of ONC-T, ONC-W1, and ONC-W2
hyb2_onc_c_strl_*yyyymmdd*.{db,xml}	List of stray light patten file names and related parameters for ONC-T
hyb2_onc_c_dist_*yyyymmdd*.{db,xml}	List of parameters related to distortion correction for ONC-T, ONC-W1, and ONC-W2
hyb2_onc_c_radc_*yyyymmdd*.{db,xml}	List of parameters related to radiometric correction for each band of ONC-T, ONC-W1, and ONC-W2. CCD sensitivity as function of CCD temperature, effective band width and band center and effective solar irradiance for each band are included.
hyb2_onc_c_phot_*yyyymmdd*.{db,xml}	List of parameters related to photometric correction for each band of ONC-T, ONC-W1, and ONC-W2
(Miscellaneous database files; not included in the bundle at now)	
hyb2_onc_c_bdpth_*yyyymmdd*.{db,xml}	List of bit depth of all images of L2a. This data set is used to fill the header of L2a images.
hyb2_onc_c_mker_*yyyymmdd*.{db,xml}	List of available SPICE meta-kernel of for each image, that can be used to create backplane (L2dbpc). The meta-kernels include spacecraft orbit and attitude kernels created as by-product during the determination of shape model (SPC or SfM) and LIDAR orbit. If none of the above meta-kernels is available, spacecraft orbit and attitude information determined by the AOCS team is used.

6.2.10.4 PSF (point spread function) data Format

The effect of point spread function (PSF) is not currently calibrated in the product pipeline process, although the method and data required for PSF-corrected might be added in a future version. The users who are willing to conduct advanced spectral analysis should note that current result of the proximity observation suggests that variation of PSF among the different wavelength causes artificial spectral change among the observations at the different altitude. More precisely, due to the object size change in the FOV with different altitudes in particular less than a few km, the relative effect of the broad PSF to the disk brightness changes. Thus, users need to be careful when producing spectra from the L2e data obtained at the altitude lower than a few km where the absolute values and the shape of the spectrum will deviate from those obtained from the data taken at Home Position (20 km). We recommend users calculate the ratios between the same areas taken at the low altitude and the high altitude such as 5-20 km, for each band, and multiplying the ratios to the low altitude data for the moment.

6.3 Label and Header Descriptions

All ONC data products contain date and time information that can be used to sort and correlate the ONC data with the products from other instruments. FITS file header information or metadata is duplicated in the PDS4 XML label to enable analyses in either standard FITS tools or PDS4 tools. Data product labels are in XML format and are PDS4 compliant.

7 Applicable Software

7.1 Utility Programs

At the current time, the Hayabusa2 project has no plans to release any mission specific utility programs.

7.2 Applicable PDS Software Tools

Data products found in the Hayabusa2 archive can be viewed with any PDS4 compatible software utility. A listing of these tools can be found at https://pds.nasa.gov/tools/about/. Hayabusa2 image data and portions of the spectrometer data are formatted as FITS data files, which can be read by any FITS compatible viewer or library function.

7.3 Software Distribution and Update Procedures

As no Hayabusa2 specific software will be released to the public, this section is not applicable.

8 Appendices

8.1 References

Bell, J. F. et al., In-flight calibration and performance of the Mars Exploration Rover Panoramic Camera (Pancam) instruments, *J. Geophys. Res.*, **111** (E2) (CiteID E02S03), https://doi.org/10.1029/2005JE002444, 2006

Hapke, B., Bidirectional reflectance spectroscopy: 1. Theory, *J. Geophys. Res.*, **86**, 3039, https://doi.org/10.1029/JB086iB04p03039, 1981

Hapke, B., Bidirectional reflectance spectroscopy: 3. Correction for macroscopic roughness, *Icarus*, **59**, 41-59, https://doi.org/10.1016/0019-1035(84)90054-X, 1984.

Hapke, B., Theory of reflectance and emittance spectroscopy, Cambridge University Press, https://doi.org/10.1017/CBO9781139025683, 2012.

Hirata, Naru, plate_renderer, The University of Aizu, https://arcspace.jp/plate_renderer:top, 2018.

Hirata, Naru, Ryugu Coordinate System Description, JAXA Data Archives and Transmission System, urn:jaxa:darts:hyb2:document:ryugu_coord_desc, 2020.

Ishiguro, M. et al., The Hayabusa Spacecraft Asteroid multi-band imaging Camera (AMICA), *Icarus*, **207**, 714-731, https://doi.org/10.1016/j.icarus.2009.12.035, 2010.

Kameda, S. et al., Detectability of hydrous minerals using ONC-T camera onboard the Hayabusa2 spacecraft, *Advances in Space Research*, **56**, 7, 1519-1524, https://doi.org/10.1016/j.asr.2015.06.037, 2015.

Kameda, S. et al., Preflight Calibration Test Results for Optical Navigation Camera Telescope (ONC-T) Onboard the Hayabusa2 Spacecraft, *Space Science Reviews*, **208**:17-31, https://doi.org/10.1007/s11214-015-0227-y, 2017.

Kameda, S. et al., Improved method of hydrous mineral detection by latitudinal distribution of 0.7-μm surface reflectance absorption on the asteroid Ryugu, *Icarus*, **360**, 114348, https://doi.org/10.1016/j.icarus.2021.114348, 2021.

Kouyama, T. et al., Post-arrival calibration of Hayabusa2's optical navigation cameras (ONCs): Severe effects from touchdown events, *Icarus*, **360**, 114353, https://doi.org/10.1016/j.icarus.2021.114353, 2021a.

Kouyama, T. et al., Image registration for multi-band images taken by ONC-T onboard Hayabusa2, arXiv:2112.09404, https://doi.org/10.48550/arXiv.2112.09404, 2021b.

Murchie, S., et al., Inflight calibration of the NEAR multispectral imager, *Icarus*, **140**, 66–91, https://doi.org/10.1006/icar.2001.6746, 1999.

Ogohara K., et al: Automated cloud tracking system for the Akatsuki Venus Climate Orbiter data. *Icarus*, **217**, 661-668, https://doi.org/10.1016/j.icarus.2011.05.017, 2012.

Pence, W. D. et al., Definition of the Flexible Image Transport System (FITS), version 3.0, *A&A*, **524**, A42, https://doi.org/10.1051/0004-6361/201015362, 2010.

Rivkin, A. S., Howell, E.S., Vilas, F., and Lebofsky, L.A., Hydrated minerals on asteroids: the astronomical record, in Asteroids III, ed. by W. Bottke, A. Cellino, P. Paolicchi, R.P. Binzel, University of Arizona Press, Tucson, 235–253, 2004.

Rosenfeld, A., and Vanderbrug, G. J.: Coarse-Fine Template Matching, IEEE. Transactions on Systems, Man and Cybernetics, 7, 104-107, https://doi.org/10.1109/TSMC.1977.4309663, 1977.

Sugita, S. et al., Hayabusa-2 ONC Science Team, Science observations strategy for HAYABUSA-2 optical navigation cameras (ONC), in Lunar Planet. Sci. Conf., vol. XXXXIII, #3026, pp. 2, 2013.

Sugita, S. et al., The geomorphology, color, and thermal properties of Ryugu: Implications for parent-body processes, *Science*, **263**, 6437, https://doi.org/10.1126/science.aaw0422, 2019.

Suzuki, H. et al., Initial inflight calibration for Hayabusa2 optical navigation camera (ONC) for science observations of asteroid Ryugu, *Icarus*, **300**:341-359, https://doi.org/10.1016/j.icarus.2017.09.011, 2018.

Tanimoto, S. L. and Pavlidis, T.: A hierarchical data structure for picture processing, *Computer Graphics and Image Processing*, **4**, 104-119, https://doi.org/10.1016/S0146-664X(75)80003-7, 1975.

Tatsumi, E. et al., Updated inflight calibration of Hayabusa2's optical navigation camera (ONC) for scientific observations during the cruise phase, *Icarus*, **325**, 153-195, https://doi.org/10.1016/j.icarus.2019.01.015, 2019a.

Tatsumi, E. et al., Updated flat-fields of ONC-T/Hayabusa2 based on close encounter with Ryugu, 50th Lunar and Planetary Science Conference 2019, #1743, pp. 2, 2019b.

Tatsumi, E. et al., Global photometric properties of (162173) Ryugu, *A&A*, **639**, A83, https://doi.org/10.1051/0004-6361/201937096, 2020.

Zellner, F., Tholen, D. J., and Tedesco, E. F., The eight-color asteroid survey: results for 589 minor planets, *Icarus*, **61**, 1355, https://doi.org/10.1016/0019-1035(85)90133-2, 1985.

8.2 Definitions of Data Processing Levels

PDS4 Data Processing Levels (From PDS Policy on Data Processing Levels (2013-03-11):

Telemetry: An encoded byte stream used to transfer data from one or more instruments to temporary storage where the raw instrument data will be extracted.

Raw: Original data from an instrument. If compression, reformatting, packetization, or other translation has been applied to facilitate data transmission or storage, those processes will be reversed so that the archived data are in a PDS approved archive format.

Partially Processed: Data that have been processed beyond the raw stage but which have not yet reached calibrated status.

Calibrated: Data converted to physical units, which makes values independent of the instrument.

Derived: Results that have been distilled from one or more calibrated data products (for example, maps, gravity or magnetic fields, or ring particle size distributions). Supplementary data, such as calibration tables or tables of viewing geometry, used to interpret observational data should also be classified as ‘derived’ data if not easily matched to one of the other three categories.

8.3 Example Calibration Data files

Example of current calibration data files are shown in Figure 21, Figure 22, Figure 23, Figure 24, Figure 25, Figure 26, Figure 27, Figure 28, Figure 29, and Figure 30.

```
# hyb2_onc_c_all_20200814.db
#
# Date: 20200814
# Creator: ONC team
# Reference:  Tatsumi et al., 2019, Kouyama et al., 2021,
#
# Calibration files for  Hayabusa2 ONC pipeline processing from L2a to L2e
#
# @attribute
# FITS keyword for calibration file
# filename
# @data
FLATCFN, hyb2_onc_c_flat_20200814.db
ELCRCFN, hyb2_onc_c_elec_20190131.db
LINCRCFN,hyb2_onc_c_linc_20190131.db
DISTCFN, hyb2_onc_c_dist_20190131.db
RADCCFN, hyb2_onc_c_radc_20190131.db
CCDTDCFN,hyb2_onc_c_radc_20190131.db
PHOTOCFN,hyb2_onc_c_phot_20190131.db
```

Figure 21. Example of calibration file list (hyb2_onc_c_all_20200814.db).

```
# hyb2_onc_c_flatfield_20200814.db
#
# Date: 20200814
# Creator: ONC team
# References:
#    [1] Suzuki et al., 2018
#    [2] Tatsumi et al., 2019
#
# Parameter and files related to create normalized flatfield.
#
#    I_flat(band, T_CCD) = I_flat(band, -29 degC) + I_flat' * Cflat * (T_ccd+29)
#
# @attribute
# Band
# FlatFileDirectoy
# I_flat(band, -29 degC) : Flatfield file for -29 degC obtained through onboard
calibration
# I_flat' : Temperature dependent component of Flatfield obtained through onboard
calibration@data
# Coefficient concerning with CCD temperature
# @data
tu,flatfield,hyb2_onc_c_flat_bse_tuf_t_v03_20190131.fit,,0
tb,flatfield,hyb2_onc_c_flat_bse_tbf_t_v03_20190131.fit,,0
tv,flatfield,hyb2_onc_c_flat_bse_tvf_f_v03_20190131.fit,,0
tn,flatfield,hyb2_onc_c_flat_bse_tnf_t_v03_20190131.fit,,0
tw,flatfield,hyb2_onc_c_flat_bse_twf_t_v03_20190131.fit,,0
tx,flatfield,hyb2_onc_c_flat_bse_txf_t_v03_20190131.fit,hyb2_onc_c_flat_pc1_txf_t_v03_2020
0814.fit,0.0661
tp,flatfield,hyb2_onc_c_flat_bse_tpf_t_v03_20190131.fit,hyb2_onc_c_flat_pc1_tpf_t_v03_2020
0814.fit,0.0503
ti,flatfield,hyb2_onc_c_flat_bse_tvf_f_v03_20190131.fit,,0
tp,flatfield,hyb2_onc_c_flat_bse_tpf_t_v03_20190131.fit,,0
w1,flatfield,hyb2_onc_c_flat_bse_w1f_f_v03_20190131.fit,,0
w2,flatfield,hyb2_onc_c_flat_bse_w2f_f_v03_20190131.fit,,0
```

Figure 22. Example of calibration file for flat correction (hyb2_onc_c_flat_20200814.db).

```
# hyb2_onc_c_elec_20190131.db
#
# Date: 20190131
# Creator: ONC team
# Reference:
#     [1] Suzuki et al., 2018,
#     [2] Tatsumi et al., 2019.
#
# Parameters required for four types of parameters related to electric circuits are
included.
# Parameters of (2), (3), (4) are used to in creation of ONC L2b images.
#
#   (1)  a/d conversion adu  [e-/count]  (Table A1 of [2])
#
#   (2)  Bias
#          ONC-T (equation 3.5 and 3.6 in [2])
#            I_bias [count/s]
#               =   ( b0 + b1 * T_(CCD,T) + b2 * T_(ELE,T) )
#                  *( b3 + b4 * T_AE )
#
#          ONC-W1, ONC-W2 (equation 5.1 in [2])
#            I_bias [count/s]
#               =   ( c0 + c1 * T_AE + c2 * T_AE**2 ) * T_(CCD,W1 or W2)
#                 + ( c3 + c4 * T_AE + c5 * T_AE**2 )
#
#        Note: the value -999 means "not applicable".
#
#   (3)  Dark signal (equation 3.7 in [2])
#           I_dark [count/s] = exp( d0 + d1 * T_(CCD,T or W1 or W2) )
#
#        Note: Values for W1 and W2 are filled tentatively with values for T.
#
#   (4)  CCD vertical transfer time per pixel
#           t_vct_pixel [s/pixel]
#
# @attribute
# Camera
# AD_conversion_unit
# b0
# b1
# b2
# b3
# b4
# c0
# c1
# c2
# c3
# c4
# c5
# d0
# d1
# t_vct_pixel
# @data
# cam,gain,  b0,   b1,    b2,   b3,      b4,   c0,      c1,     c2,  c3,   c4,     c5,
d0,  d1,t_vct_pixel
T, 20.95,320.66,0.652,-0.953,0.987,-0.00251, -999,    -999,   -999,-999, -999,   -
999,0.52,0.10,7.460e-6
W1,20.86,  -999, -999,  -999, -999,    -999,0.680,-5.74e-3,1.06e-4, 260,-1.72,8.50e-
3,0.52,0.10,7.000e-6
W2,20.11,  -999, -999,  -999, -999,    -999,0.573,-2.95e-3,8.92e-3, 288,-1.65,6.29e-
3,0.52,0.10,7.200e-6
```

Figure 23. Example of calibration file for hardware correction (hyb2_onc_c_elec_20190131.db).

```
# hyb2_onc_c_linc_20190131.db
#
# Date: 20190131
# Creator: ONC team
# References:
#    [1] Tatsumi et al., 2019
#
# Parameters are described in [1] but these are not used at now.
#
# Parameter Non-linearity correction in
#
#  I' [count/sec] = c0 + c1 * I +  c2 * I^2 + c3 * I^3 + c4 * I^4
#
# @attribute
# Camera
# c0
# c1
# c2
# c3
# c4
# @data
#cam,c0,c1,c2,c3,c4
T, 0,1,0,0,0
W1,0,1,0,0,0
W2,0,1,0,0,0
```

Figure 24. Example of calibration file for linearity correction (hyb2_onc_c_linc_20190131.db).

```
# hyb2_onc_c_strl_20190131.db
#
# Date: 20190131
# Creator: ONC team
# References:
#    [1] Suzuki et al., 2018
#    [2] Tatsumi et al., 2019.
#
# Parameter and files related to stray light removal.
#
# When phi < -7 degrees or gamma > -10 degrees (note that this model is
# not applicable when gamma < -3 degrees) is negligible, otherwise stray light component
is:
#
#    (I_sl * t_exp)/R_sol^2
#
# where
#
#    t_exp is the exposure time in seconds,
#    R_sol is the solar distance in au, and
#    I_sl is the model stray light image,
#
# The model stray light image is:
#
#    I_sl = i_sl * M_sl
#
# where
#
#    i_sl is the intensity of stray light, and
#    M_sl is the stray light pattern in the field of view.
#
# These two variable are further expressed by
#
#   i_sl = ( -0.0879 * phi^3 - 5.61 * phi^2 - 119.4 * phi - 603.8 )
#          * ( -0.0037 * gamma^2 + 0.113 * gamma + 0.956 ),
#
#   M_sl = M_ave + ( 0.02105 * phi^2 + 1.338 * phi + 17.02 ) * M_PC1,
#
# where phi and gamma are the angle between Hayabusa2-Sun vector and Z_SC
# and the twisting angle around Z_SC, M_ave is the stray light mean
# component and M_PC1 is the first component of the stray light of the
# principal component analysis.
#
# @attribute
# Band
# straylight mean pattern file
# straylight pc1 pattern file
# straylight pc2 pattern file
# @data
ta,hyb2_onc_c_strl_mea_taf_f_v01_20190131.fit,hyb2_onc_c_strl_pc1_taf_f_v01_20190131.fit,h
yb2_onc_c_strl_pc2_taf_f_v01_20190131.fit
```

Figure 25. Example of calibration file for stray light correction (hyb2_onc_c_strl_20190131.db).

```
# hyb2_onc_c_dist_20190131.db
#
# Date: 20190131
# Creator: ONC team
# References:
#    [1] Suzuki et al., 2018
#    [2] Tatsumi et al., 2019
#
# Three types of Parameters on distortion and offset of optics are included.
# Used in creation of L2c.
#
# (1) Alignment offset (obtained from star observations)
#
#     (h, v) in the unit of pixel in the image coordinates.
#
#     (Table 6.1 in [2])
#
#
# (2) Parameters for distortion correction function "dist" in
#
#     R' = a0 + a1 * R + a2 * R^2 + a3 * R^3 + a4 * R^4 + a5 * R^5
#
#     (Table 2 in [1] for ONC-W1 and ONC-W2, Table 6.1 in [2])
#
#
# (3) Parameters for inverse of distortion correction function "dist^-1" in
#
#     R = b0 + b1 * R' + b2 * R'^2 + b3 * R'^3 + b4 * R'^4 + b5 * R'^5
#
# @attribute
# Camera
# Alignment offset h
# Alignment offset v
# a0
# a1
# a2
# a3
# a4
# a5
# b0
# b1
# b2
# b3
# @data
# cam,h,    v,a0,  a1,a2,     a3,a4,       a5,b0,       b1,         b2,         b3,
b4,          b5
T,  9.5,-22.5,0,1.000,0,-9.28e-9,0,         0,0,1.00001e+0,-7.07794e-8, 9.45776e-9,
0,           0
W1,-3.5, -2.5,0,1.000,0,3.134e-7,0,-1.716e-13,0,9.99570e-1, 1.19590e-5,-4.15730e-
7,3.71770e-10,-9.07150e-14
W2, 0.5, -0.5,0,1.000,0,2.893e-7,0,-1.365e-13,0,9.99340e-1, 1.42190e-5,-3.93550e-
7,3.41040e-10,-8.54530e-14
```

Figure 26. Example of calibration file for alignment offset and distortion correction (hyb2_onc_c_dist_20190131.db).

```
# hyb2_onc_c_radc_20190131.db
#
# Date: 20190131
# Creator: ONC team
# References:
#     [1] Tatsumi et al., 2019
#     [2] Kouyama et al., 2021
#
# The parameters related to radiometric calibration in Hayabusa2 ONC
# L2c and L2d creation are listed in the below.
# These values are defined for each camera.
# In the case of ONC-T, they are defined for each band.
#
# (1) Effective band center for each camera [um].
#
# (2) Effective bandwidth for each camera [um].
#
# (3) Effective solar irradiance in [W/m^2/um)]
#
# (4) Effective sensitivity in [count/sec/(W/sr/m^2/um)]
#
#     The sensitivity is defined by the following equation:
#
#        S = S0(period) * { 1 + S1(period) * ( t - t_start(period) ) }
#            * ( a_CCD * (T_CCD + 30 degrees Celsius) + 1 )
#
#     where
#              t: time in days,
#          T_CCD: CCD temperature in degrees Celsius,
#       period 1: before TD1,
#       period 2: between TD1 and TD2,
#       period 3: after TD2.
#
# @attribute
# Bands
# Effective band center for each camera bc [um].
# Effective bandwidth for each camera bw [um].
# Effective solar irradiance in  [W/m^2/um)]
# a_CCD. No data for ONC-T wide, w1 and w2. ONC-T V band value is used for the moment as the
representative values.
# Parameters for sensitivity for period 1: t_start_in_YYYY-MM-DDThh:mm:ssZ(1),S0(1),S1(1)
# Parameters for sensitivity for period 2: t_start_in_YYYY-MM-DDThh:mm:ssZ(2),S0(2),S1(2)
# Parameters for sensitivity for period 3: t_start_in_YYYY-MM-DDThh:mm:ssZ(3),S0(3),S1(3)
# @data
#band, bc,    bw, irrad,      a_CCD,{period 1: t_start, S0, S1},  {period 2: t_start, S0, S1},
{period 3: t_start, S0, S1}
tu,0.3975,0.0347,1343.7,  -0.001449,2014-12-03T04:22:04Z,439.1, 0,2019-02-21T22:29:13Z,410.1,
0,2019-07-11T01:06:22Z,399.7, -2.52e-4
tb,0.4798,0.0267,1969.1,  -0.000968,2014-12-03T04:22:04Z,969.0, 0,2019-02-21T22:29:13Z,899.1,
0,2019-07-11T01:06:22Z,879.6, -2.52e-4
tv,0.5489,0.0279,1859.7,  -0.000814,2014-12-03T04:22:04Z,1175.0,0,2019-02-
21T22:29:13Z,1092.8,0,2019-07-11T01:06:22Z,1071.2,-2.52e-4
tn,0.5899,0.0116,1788.0,  -0.000866,2014-12-03T04:22:04Z,546.9, 0,2019-02-21T22:29:13Z,510.9,
0,2019-07-11T01:06:22Z,498.3, -2.52e-4
tw,0.7001,0.0288,1414.4,  -0.000355,2014-12-03T04:22:04Z,1515.0,0,2019-02-
21T22:29:13Z,1418.9,0,2019-07-11T01:06:22Z,1380.5,-2.52e-4
tx,0.8573,0.0424,985.8,   -0.001771,2014-12-03T04:22:04Z,1499.8,0,2019-02-
21T22:29:13Z,1405.8,0,2019-07-11T01:06:22Z,1373.5, -2.52e-4
tp,0.9451,0.0572,834.9,   -0.004201,2014-12-03T04:22:04Z,961.2, 0,2019-02-21T22:29:13Z,898.9,
0,2019-07-11T01:06:22Z,882.6, -2.52e-4
ti,0.6168,0.400, 29141.10,-0.000814,2014-12-03T04:22:04Z,18412, 0,2019-02-21T22:29:13Z,17124,
0,2019-07-11T01:06:22Z,16786, -2.52e-4
w1,0.5749,0.170, 2184.16, -0.000814,2014-12-03T04:22:04Z,1.38e3,0,2019-02-21T22:29:13Z,5.2e2,
0,2019-07-11T01:06:22Z,5.0e2, 0
w2,0.5672,0.170, 6077.66, -0.000814,2014-12-03T04:22:04Z,3.84e3,0,2019-02-
21T22:29:13Z,3.84e3,0,2019-07-11T01:06:22Z,3.84e3,0
```

Figure 27. Example of calibration file for radiometric correction (hyb2_onc_c_radc_20190131.db).

```
# hyb2_onc_c_phot_20190131.db
#
# Date: 20190131
# Creator: ONC team
# Reference:
#     [1] Tatsumi et al., 2020
#
# The parameters related to photometric correction in Hayabusa2 ONC
# L2e creation are listed in the below. Since the values for ti, w1,
# and w2 are not obtained, values of these band are filled by the
# values from other bands.
# @attribute
# band
# Hapke model parameter w
# Hapke model parameter g
#   (signature of this parameter is different from ones in [1],
#    because of the difference of the definition of equation in SIS)
# Hapke model parameter B0
# Hapke model parameter h
# Hapke model parameter thetabar (deg)
# @data
#band, w,     g,  B0,    h,thetabar (deg)
tu,0.047,-0.386,0.98,0.075,28
ub,0.045,-0.388,0.98,0.075,28
uv,0.044,-0.388,0.98,0.075,28
un,0.044,-0.387,0.98,0.075,28
tw,0.045,-0.388,0.98,0.075,28
tx,0.047,-0.374,0.98,0.075,28
tp,0.046,-0.377,0.98,0.075,28
ti,0.044,-0.388,0.98,0.075,28
w1,0.044,-0.388,0.98,0.075,28
w2,0.044,-0.388,0.98,0.075,28
```

Figure 28. Example of calibration file for photometric correction (hyb2_onc_c_ phot_20190131.db).

```
# hyb2_onc_c_bdpth_20200930.db
#
# Date: 20200930
# Creator: ONC team
# Reference:  NON
#
#  List of bit depth of all images of L2a. This data set is used to fill the header of
   L2a images.
# @attribute
# image file name: string
# bit depth : integer
# @data
hyb2_onc_20190221_220115_w1b_l2a.fit,8
hyb2_onc_20190221_220115_w1f_l2a.fit,8
hyb2_onc_20190221_220218_w1b_l2a.fit,10
hyb2_onc_20190221_220218_w1f_l2a.fit,10
hyb2_onc_20190221_220322_tvb_l2a.fit,10
hyb2_onc_20190221_220322_tvf_l2a.fit,10
hyb2_onc_20190221_220426_w1b_l2a.fit,10
hyb2_onc_20190221_220426_w1f_l2a.fit,10
hyb2_onc_20190221_220530_tvb_l2a.fit,10
hyb2_onc_20190221_220530_tvf_l2a.fit,10
hyb2_onc_20190221_222815_w1b_l2a.fit,12
hyb2_onc_20190221_222815_w1f_l2a.fit,12
hyb2_onc_20190221_222816_w1b_l2a.fit,12
…
```

Figure 29. Example of bit depth database file (hyb2_onc_c_bdpth_20200930.db).

```
# hyb2_onc_c_mker_20200930.db
#
# Date: 20200930
# Creator: ONC team
# Reference:  NON
#
#  List of available SPICE meta-kernel of for each image, that can be used to create
   backplane (L2dbpc).
#  The meta-kernels include spacecraft orbit and attitude kernels created as by-product
   during the
#  determination of shape model (SPC or SFM) and LIDAR orbit. If none of the above meta-
   kernels is
#  available, spacecraft orbit and attitude information determined by AOCS team is used
   (.
# @attribute
# image file name: string
# meta-kernel index : string
# @data
hyb2_onc_20190221_220115_w1b_l2a.fit,SPC20200323
hyb2_onc_20190221_220115_w1f_l2a.fit,SPC20200323
hyb2_onc_20190221_220218_w1b_l2a.fit,SPC20200323
hyb2_onc_20190221_220218_w1f_l2a.fit,SPC20200323
hyb2_onc_20190221_220322_tvb_l2a.fit,SPC20200323
hyb2_onc_20190221_220322_tvf_l2a.fit,SPC20200323
hyb2_onc_20190221_220426_w1b_l2a.fit,SPC20200323
hyb2_onc_20190221_220426_w1f_l2a.fit,SPC20200323
hyb2_onc_20190221_220530_tvb_l2a.fit,SPC20200323
hyb2_onc_20190221_220530_tvf_l2a.fit,SFM20200815
hyb2_onc_20190221_222815_w1b_l2a.fit,SFM20200815
hyb2_onc_20190221_222815_w1f_l2a.fit,LIDARYYMMDD
hyb2_onc_20190221_222816_w1b_l2a.fit,ANALYSISYYMMDD
…
```

Figure 30. Example of SPICE kernel database file (hyb2_onc_c_mker_20200930.db).

8.4 PDS4 attribute and FITS keyword of the parameters used for calibration

Table 28. PDS4 attribute and FITS keyword of the parameters used for calibration.

Parameters	Description	PDS4 attribute	FITS keyword	Calibration equation No.
$T_{\mathrm{CCD,T}}$	The temperature of the CCD of ONC-T in degC	hyb2:ONC_Instrument_Attributes/hyb2:t_ccd_temperature	T_CCDT	(2), (5), (8), (21)
$T_{\mathrm{CCD,W1}}$	The temperature of the CCD of ONC-W1 in degC	hyb2:ONC_Instrument_Attributes/hyb2:w1_ccd_temperature	W1_CCDT	(2), (5), (8), (21)
$T_{\mathrm{CCD,W2}}$	The temperature of the CCD of ONC-W2 in degC	hyb2:ONC_Instrument_Attributes/hyb2:w2_ccd_temperature	W2_CCDT	(2), (5), (8), (21)
$T_{\mathrm{ELE,T}}$	The temperature of the sensor head electronics of ONC-T in degC	hyb2:ONC_Instrument_Attributes/hyb2:t_electric_circuit_temperature	T_ELET	(2)
$T_{\mathrm{ELE,W1}}$	The temperature of the sensor head electronics of ONC-W1 in degC	hyb2:ONC_Instrument_Attributes/hyb2:w1_electric_circuit_temperature	W1_ELET	(2)
$T_{\mathrm{ELE,W2}}$	The temperature of the sensor head electronics of ONC-W2 in degC	hyb2:ONC_Instrument_Attributes/hyb2:w2_electric_circuit_temperature	W2_ELET	(2)
T_{AE}	The temperature of ONC-AE in degC	hyb2:ONC_Instrument_Attributes/hyb2:onc_analog_electronics_temperature	ONC_AET	(2)
t_{EXP}	The exposure time in seconds	hyb2:Image_Observation_Information/hyb2:exposure_duration	XPOSURE	(5), (6), (11), (22)
R_{sol}	Solar distance used for calibration in AU	hyb2:ONC_Image_Processing_Parameters/hyb2:solar_distance_for_calibration	SOLDCAL	(11), (23)

8.5 *Definition of mission phase and operation type*

Table 29. Definition of mission phase

Start Date/Time	**Abbreviation**	**Name of mission phase**
2014-12-03T04:22:04Z	commissioning	Commissioning Phase
2015-03-03T00:00:00Z	edvega	EDVEGA Phase
2015-10-01T00:00:00Z	earth_swing-by	Earth Swing-by Phase
2015-12-22T14:10:00Z	transfer	Transfer Phase
2018-06-03T05:59:00Z	approach	Approach Phase
2018-06-27T00:35:00Z	proximity	Asteroid Proximity Phase
2019-11-13T01:00:00Z	return	Return Phase

Table 30. Definition of Operation

Date/Time (UTC)	**Description**
2018-06-27T00:35:00	start of the Asteroid Proximity Phase
2018-07-17 – 2018-07-25	BOX-C operation (BOX-C-1)
2018-07-31 – 2018-08-02	Mid-altitude descent observation (MID)
2018-08-05 – 2018-08-10	Gravity measurement descent operation (GRV)
2018-08-18 – 2018-09-07	BOX-B operation (BOX-B-1 and BOX-B-2)
2018-09-10 – 2018-09-12	Touch-down #1 Rehearsal 1 (TD1-R1)
2018-09-19 – 2018-09-21	MINERVA-II1 deployment operation (MNRV1)
2018-09-30 – 2018-10-04	MASCOT deployment operation (MSC)
2018-10-14 – 2018-10-16	Touch-Down #1 Rehearsal 1A (TD1-R1-A)
2018-10-23 – 2018-10-25	Touch-Down #1 Rehearsal 3 (TD1-R3)
2018-10-27 – 2018-11-05	BOX-C operation (BOX-C-2 and BOX-C-3)
2018-11-23 – 2018-12-29	Conjunction Orbit Operation
2019-01-06 – 2019-01-13	BOX-B operation (BOX-B-3)
2019-01-19 – 2019-01-31	BOX-B operation (BOX-B-4)
2019-02-20 – 2019-02-22	Touch Down #1 (TD1-L08E1)
2019-02-23 – 2019-03-01	BOX-C operation (BOX-C-4)
2019-03-05 – 2019-03-08	Low Altitude Descent Observation (DO-S01)
2019-03-19 – 2019-03-22	Crater search descent pre-impact operation (CRA1)
2019-04-02 – 2019-04-05	Small Carry-on Impactor operation (SCI)
2019-04-23 – 2019-04-25	Crater search descent post-impact operation (CRA2)
2019-05-13 – 2019-05-16	Pin-point Touchdown Rehearsal 1 (PPTD-TM1)
2019-05-27 – 2019-05-30	Pin-point Touchdown Rehearsal 1A (PPTD-TM1A)
2019-06-11 – 2019-06-13	Pin-point Touchdown Rehearsal 1B (PPTD-TM1B)
2019-07-08 – 2019-07-11	Pin-point Touchdown operation (PPTD)
2019-07-20 – 2019-07-31	BOX-C operation (BOX-C-5)
2019-08-08 – 2019-08-27	BOX-B operation (BOX-B-5 and BOX-B-6)
2019-09-11 – 2019-09-17	Target Markers orbiting operation (TM-ORB)
2019-09-23 – 2019-09-27	BOX-B operation (BOX-B-7)
2019-09-28 – 2019-10-08	MINERVA-II2 orbiting operation (MNRV-ORB)
2019-10-08 – 2019-10-14	BOX-C operation (BOX-C-6)
2019-10-19 – 2019-10-30	BOX-C operation (BOX-C-7)
2019-11-13T01:00:00	end of the Asteroid Proximity Phase